New Jersey Institute of Technology
Digital Commons @ NJIT

Dissertations | Electronic Theses and Dissertations

Fall 1-31-1998

FLAG : the fault-line analytic graph and fingerprint classification

Ching-Yu Huang
New Jersey Institute of Technology

Follow this and additional works at: https://digitalcommons.njit.edu/dissertations

 Part of the Computer Sciences Commons

Recommended Citation

Huang, Ching-Yu, "FLAG : the fault-line analytic graph and fingerprint classification" (1998). *Dissertations*. 947.
https://digitalcommons.njit.edu/dissertations/947

This Dissertation is brought to you for free and open access by the Electronic Theses and Dissertations at Digital Commons @ NJIT. It has been accepted for inclusion in Dissertations by an authorized administrator of Digital Commons @ NJIT. For more information, please contact digitalcommons@njit.edu.

Copyright Warning & Restrictions

The copyright law of the United States (Title 17, United States Code) governs the making of photocopies or other reproductions of copyrighted material.

Under certain conditions specified in the law, libraries and archives are authorized to furnish a photocopy or other reproduction. One of these specified conditions is that the photocopy or reproduction is not to be "used for any purpose other than private study, scholarship, or research." If a, user makes a request for, or later uses, a photocopy or reproduction for purposes in excess of "fair use" that user may be liable for copyright infringement,

This institution reserves the right to refuse to accept a copying order if, in its judgment, fulfillment of the order would involve violation of copyright law.

Please Note: The author retains the copyright while the New Jersey Institute of Technology reserves the right to distribute this thesis or dissertation

Printing note: If you do not wish to print this page, then select "Pages from: first page # to: last page #" on the print dialog screen

NJIT
New Jersey's Science & Technology University

The Van Houten library has removed some of the personal information and all signatures from the approval page and biographical sketches of theses and dissertations in order to protect the identity of NJIT graduates and faculty.

ABSTRACT

FLAG: THE FAULT-LINE ANALYTIC GRAPH AND FINGERPRINT CLASSIFICATION

by
Ching-Yu Huang

Fingerprints can be classified into millions of groups by quantitative measurements of their new representations - Fault-Line Analytic Graphs (FLAG), which describe the relationship between ridge flows and singular points. This new model is highly mathematical, therefore, human interpretation can be reduced to a minimum and the time of identification can be significantly reduced.

There are some well known features on fingerprints such as singular points, cores and deltas, which are global features which characterize the fingerprint pattern class, and minutiae which are the local features which characterize an individual fingerprint image. Singular points are more important than minutiae when classifying fingerprints because the geometric relationship among the singular points decide the type of fingerprints.

When the number of fingerprint records becomes large, the current methods need to compare a large number of fingerprint candidates to identify a given fingerprint. This is the result of having a few synthetic types to classify a database with millions of fingerprints. It has been difficult to enlarge the number of classification groups because there was no computational method to systematically describe the geometric relationship among singular points and ridge flows. In order to define a more efficient classification method, this dissertation also provides a systematic approach to detect singular points with almost pinpoint precision of 2×2 pixels using efficient algorithms.

FLAG: THE FAULT-LINE ANALYTIC GRAPH AND FINGERPRINT CLASSIFICATION

by
Ching-Yu Huang

A Dissertation
Submitted to the Faculty of
New Jersey Institute of Technology
in Partial Fulfillment of the Requirements for the Degree of
Doctor of Philosophy

Department of Computer and Information Science

January 1998

APPROVAL PAGE

FLAG: THE FAULT-LINE ANALYTIC GRAPH AND FINGERPRINT CLASSIFICATION

Ching-Yu Huang

12/9/97

Dr. DaoChuan Hung, Advisor and Chair — Date
Associate Professor of Computer and Information Science, NJIT

12/9/97

Dr. James A. McHugh, Committee Member, — Date
Chairperson and Professor of Computer and Information Science, NJIT

12/9/97

Dr. Peter A. Ng, Committee Member, — Date
Professor of Computer and Information Science, NJIT

12/9/97

Dr. Frank Y. Shih, Committee Member, — Date
Associate Professor of Computer and Information Science, NJIT

12/9/97

Dr. Nirwan Ansari, Committee Member, — Date
Professor and Associate Chair for Graduate Studies,
Electrical and Computer Engineering, NJIT

12/9/97

Dr. Frederic P. Fischer, Committee Member, — Date
President of Sequential Data Systems

BIOGRAPHICAL SKETCH

Author: Ching-Yu Huang

Degree: Doctor of Philosophy in Computer Science

Date: January 1998

Date of Birth:

Place of Birth:

Undergraduate and Graduate Education:

- Doctor of Philosophy in Computer Science,
  New Jersey Institute of Technology, Newark, NJ, 1998
- Master of Science in Computer Science,
  New Jersey Institute of Technology, Newark, NJ, 1993
- Bachelor of Engineering in Computer Science and Engineering,
  Tamkang University, Taipei, Taiwan, 1990

Major: Computer and Information Science

Presentations and Publications:

D. C. Hung and Ching-Yu Huang, "On the Detection of the Center of A Convergence," *Second Asian Conf. on Computer Vision*, Singapore, Dec. 5 - 8, 1995.

D. C. Hung and Ching-Yu Huang, "A Model for Detecting Singular Points of a Fingerprint," in *Proceedings of 9th Florida Artificial Intelligence Research Symposium (FLAIRS '96)*, Florida AI Research Society, Key West, Florida, pp. 44 - 448, May 20 - 22, 1996.

D. C. Hung, Ching-Yu Huang and Jane H. Cheng, "A New Model for Representing and Retrieving Structural Patterns," in *Proceedings of the 5th International Conference on Intelligent Systems (IS '96)*, International Society for Computers and Their Applications (ISCA), Reno, Nevada, pp. 98 - 101, Jun. 19 - 21, 1996.

BIOGRAPHICAL SKETCH
(Continued)

D. C. Hung and Ching-Yu Huang, "A Syntactic Model for Pattern Recognition," in *Proceedings of the International Association of Science And Technology for Development (IASTED) International Conference on Artificial Intelligence, Expert Systems and neural Networks*, Honolulu, Hawaii, Aug. 19-22, 1996.

D. C. Hung, Ching-Yu Huang and Jane H. Cheng, "Detecting Fingerprint Singular Points by A Hierarchical Model," *Proceedings of 7th International Conference on Signal Processing Applications & Technology (ICSPAT '96)*, Miller Freeman, Inc., Boston, Massachusetts, pp. 1153 - 1157, Oct. 7 - 10, 1996.

D. C. Hung, Ching-Yu Huang and Jane H. Cheng, "A Fuzzy Technique for Flow Oriented Image Direction Computing," *Proceedings of Artificial Neural Networks in Engineering (ANNIE '96)*, University of Missouri - Rolla, St. Louis, Missouri, pp. 519 - 524, Nov. 10 - 13, 1996.

Ching-Yu Huang, D. C. Hung and Jane H. Cheng, "The SPFL-Graph with Pattern Modeling of Fingerprints," *Proceedings of Sixth Workshop on Digital Image Processing and Computer Graphics (DIP'97)*, Vienna, Austria, Oct. 20 - 22, 1997.

Ching-Yu Huang, D. C. Hung, "On the Automatic Preprocessing of Fingerprints," submitted to *1998 IEEE Southwest Symposium On Image Analysis and Interpretation (SSIAI'98)*, Tucson, Arizona, April 6-7, 1998.

Ching-Yu Huang, D. C. Hung, "The Fault-Line-Analytic-Graphs and Their Normalization," submitted to *IEEE Computer Society Conference on Computer Vision and Pattern Recognition (CVPR'98)*, Santa Barbara, California, June 23-25, 1998.

Ching-Yu Huang, D. C. Hung, "The Multi-Index Model for Fingerprint Classification," submitted to *IEEE Computer Society Conference on Computer Vision and Pattern Recognition (CVPR'98)*, Santa Barbara, California, June 23-25, 1998.

This work is dedicated to
my wife, Pao-Lien and
my daughter, Grace

ACKNOWLEDGMENT

Doctoral research is arduous, but this difficult period of research was greatly mitigated by helpful faculty and colleagues in the Department of Computer and Information Science, from whom the author received encouragement. The author is grateful to friends made during this research and would like to extend special thanks to them.

First, the author would like to thank his research advisor, Professor DaoChuan Hung, for his advice and guidance during the five and a half years of his master's and doctoral research. Professor Hung's valuable help was instrumental to the author in the process of this research. The author is proud to have co-authored with him many papers for conferences and journals.

In addition, the author appreciates the help and suggestions given by Professors James McHugh, Peter Ng, Frank Shih, Nirwan Ansari and Dr. Fischer, members of the dissertation committee. Special thanks also go to the CIS Department for the financial support given during the period of this research. The author would also like to thank Jane H. Cheng, the co-author of some of the publications, Without her contribution, the publications would not have been possible.

The author appreciate the help of National Institute of Standards and Technology (NIST) for providing free fingerprint images as our testing database, and the help of the Connecticut Forensic Science Laboratory for the demonstration of the Automatic Fingerprint Identification System (AFIS) and suggestions for our research. The author also wants to thank Jerome Paris and Janet Bodner, professors of the Humanities and Social Sciences Department, Eduardo Morales, and Mark Milano, the author's brother in-law, for their enthusiastic help in English.

Finally, sincere thanks to the author's parents for their never-ending support,

understanding, and encouragement during the years of his advanced studies. The author is especially grateful to his dear wife, Pao-Lien Wang, and his daughter, Grace, for their love inspiration.

TABLE OF CONTENTS

TABLE OF CONTENTS
(Continued)

Chapter **Page**

TABLE OF CONTENTS
(Continued)

Chapter **Page**

LIST OF TABLES

Table **Page**

LIST OF FIGURES

LIST OF FIGURES
(Continued)

Figure **Page**

LIST OF FIGURES
(Continued)

Figure **Page**

CHAPTER 1

INTRODUCTION

Fingerprints probably are the most important type of physical evidence which can be used for identification [19]. A fingerprint is composed of two parts, ridges and valleys, as shown in Figure 1.1. The ridges and valleys shape into different patterns which determine the type of fingerprint. As it is well known, during the life span of a person, fingerprints remain the same. They do not fade with the passing of time. A fingerprint can be permanently changed [57] if and only if the pad of the finger is seriously hurt. Based on these characteristics, immutable, permanent, and that no two fingerprints have been found the same so far, fingerprints have been used as an unique mean of identification for people [107].

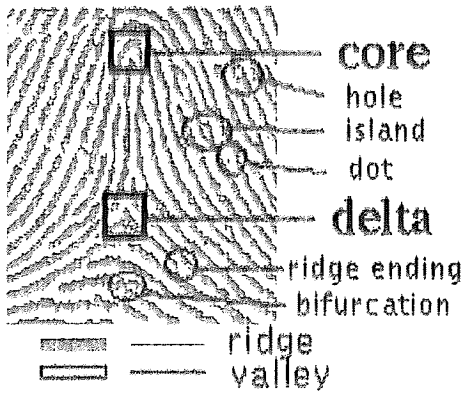

Figure 1.1 A sample of a fingerprint. Singular points, deltas and cores, are identified by squares. Minutiae are identified by circles.

Fingerprint services are supplied for criminal investigation and identification, police officer employment applications, Immigration and Naturalization Service documentation, and for other forensic identification purposes [8] [22]. Fingerprint research can be applied not only to criminal investigation but also to industry. Fingerprints are

convenient, nearly impossible to imitate, impossible to lose, and easy to trace. Fingerprints may replace handwritten signatures as the standard authentication for credit cards and personal identification cards [91]. Many building entrances and other areas of factories which need to be secure use fingerprint lockers to prevent improper access.

When identifying images, we need invariant features to compare them. There are some well known features on fingerprints such as singular points and minutiae shown in Figure 1.1. Singular points are global features which characterize the fingerprint pattern class. Minutiae are the local features which characterize an individual fingerprint image. A fingerprint has only a few singular points and many randomly distributed minutiae. Singular points are more important than minutiae when classifying fingerprints because they are global features. That is why researchers try to detect singular points to simplify the recognition process.

Kurre [24] stated that the current amount of the FBI fingerprint database is around 219 million and the total number of fingerprints increased 12.5% over the year 1996. This means that the total number of total records will more than double in less than a decade. The best way to quickly identify a fingerprint against a huge database is to classify fingerprints into a large number of groups and then match the fingerprints by the minutiae.

1.1 Motivation

When the number of fingerprints in the database is huge, the current methods are not fast enough to compare all fingerprints within a class. The reason of this is because currently there are only a few groups (less than ten) to classify fingerprints. In the FBI database, each fingerprint group contains an average of 21 millions of records which is a large number of records to be managed. The number of classification groups cannot be increased because there is no way to precisely detect singular points and to find the

relationships between them. The problem with precise identification of singular points is that the block, or the locator grid is not accurate enough. Researchers have detected, although imprecisely, singular points within a block where the area size is 16×16 pixels. The average block size is 48×48 and the worst case is an 80×80 pixels area [80] [94].

The purpose of this dissertation is to provide a systematic approach both to detect singular points and to classify fingerprints using more efficient techniques. In this dissertation, we have successfully detected singular points in almost pinpoint areas of 2×2 pixels, and at the same time we have classified them into cores and deltas. In addition to the detecting techniques, and based on the outstanding results, fingerprints can be divided into hundreds of thousands of groups which are based on the mathematic geometric relationship between cores and deltas. It is highly human independent so that ambiguous types can be reduced to a minimum. With so many classifying groups, the speed of search will increase, and the number of resulting candidates will decrease dramatically for the matching process. Our algorithms will greatly improve fingerprint technology. It is hoped that many problems of fingerprints can be solved by our proposed approaches.

1.2 The Survey of Fingerprint Fundamentals

There are several types of research related to fingerprint processing, such as fingerprint acquisition, enhancement, segmentation, thinning, edge detection, and direction computation. They are fundamental image processing techniques.

1.2.1 Image Acquisition

The acquisition type of fingerprints can be divided into passive and active.

a) Passive Method: In this method, the fingerprint is usually found on an object which may be present at a criminal scene: a desk, a wall, or any possible thing. During this process, the fingerprint is painted with some chemical powder, and then is pressed onto a

paper card [13] [105]. After the manual procedure, the card is scanned under a certain resolution and the fingerprint is transferred into a digitized image file [7]. Generally, after the fingerprint is pressed onto the paper card, the subsequent procedures depend solely on the quality of the image on the card. Normally, this passive method can be applied only once.

b) Active Method: This method gets an image directly when a fingertip presses onto a digital optic machine with a prism and a camera [25] [30] [58] [99] [102]. The machine directly transfers the image into a digitized file. The digitizing process is the same as with a scanner. The differences between this active method and the passive one are that here, the quality of the image depends on the pressure applied when the fingertip is pressed, and if the image is noisy, the user can repeat the procedure several number of times.

The FBI uses the wavelet compression technique [5] [6] [32] to store the fingerprint images to save the space under 500 dpi resolution. The wavelet compression is a lossy method which means some information in compressed images may be removed, but the method can keep the most important features such as ridges, valleys and singular points.

1.2.2 Image Enhancement

The latent fingerprint is usually noisy and need to be enhanced before it can be identified [33] [95]. If the quality is not up to an acceptable standard, fingerprint recognition becomes extremely difficult. Coetzee and Botha [15] developed some skills in enhancing low quality images of fingerprints. Hung [39] proposed a technique to connect broken ridges and remove the bridges in a skeleton fingerprint image. Sherstinsky [87] restored and enhanced fingerprint images using a novel non-linear dynamic system.

1.2.3 The Segmentation of Fingerprints

Better binary images of fingerprints are very important to later processing. Because of their latent characteristic, fingerprints are usually digitized from paper cards where the resulting images contain not only fingerprints, but also other redundant objects. NIST [10] developed a simple algorithm to extract the major parts of fingerprints from these images. The techniques of thinning, minutiae detecting, direction computing and many others require that the images contain only two gray levels, usually ridges as black and valleys as white. In addition, the thresholding process must be automatic and not dependent on human analysis.

1.2.4 Thinning and Edge Detection

The ridge counting and minutiae detecting are usually applied by thinning methods. The process of thinning is to reduce a big object into its skeleton [47] [72]. Several thinning algorithms have been proposed [2] [3] [48] [55] [88]. Edge detection can help the recognition of objects [46]. Tan and Loh [100] developed hierarchical structures for efficient edge detection. Tabbone and Ziou [97] used two scales to detect edges. Verma [101] also did edge detection on fingerprints. However, these techniques are noise-sensitive so that image quality must be good.

1.2.5 Direction Computation

The vector or directional technique is widely used in flow-oriented images such as fingerprints and optic flow because they both have the particular characteristic of direction-oriented patterns [50] [89] [90] [98] [110]. Sherlock and Monro [86] presented a simple model for interpreting fingerprint topology by using local ridge orientation of block directions and describing the topological behavior of ridge flows. The ridges or valleys can be represented as several directions which are quantized into certain numbers and computed from the neighborhood pixels [73] [103].

Mehtre [66] [67] and Srinivasan [94] computed the block direction by a major histogram within a block by a gray values difference method. In addition, Kawagoe [51] uses the gradient in the threshold image and computes the direction for each block. The result of the gray values difference method may need to be smoothed iteratively until the quality is good. The block size in their methods is highly dependent on the quality of the directional image. When the block size is larger, their method can get only rough singular point positions even though the range may be several blocks.

Fuzzy theory has proven itself to be of significant importance in pattern recognition problems. Fuzzy methods are particularly useful when it is not reasonable to assume the uncertain values [18] [54] [75]. A fuzzy technique is proposed by Hung and Huang [44] with a circular template applied to compute a better pixel-wise direction.

1.3 The Survey of Fingerprint Features

To compare two images we must have some reference points which exist in most similar images [1] [11]. The matching process is based on these extracted features [45] [59] [60]. What features are helpful and how to detect them are important for fingerprint identification. In fingerprints, there are some points which are always considered as reference points: singular points and minutiae.

1.3.1 Singular Points

Singular points are classified as deltas or cores, as shown in Figure 1.1. A delta, according to Henry [35] is ''an outer terminus: it may be formed either (a) by the bifurcation of a single ridge, or (b) by the abrupt divergence of two ridges that hitherto had run side by side.'' A core is ''an inner terminus: the core of a loop may consist either of an even or an uneven number of ridges (termed ''rods'') not joined together, or it may consist of two ridges formed together at their summit (termed ''staple'').''

Computationally, a singular point is defined as a location where a local maximum in ridge curvature is detected [84]. That is, singular points can be analytically extracted from directional patterns. The singular points are the most important landmarks in classifying a fingerprint because they are the physical centers of convergences or divergences to a ridge pattern. Detecting singular points is not only limited to two dimensions, but also can be applied in three dimensions. Sander and Zucker [85] detected singularities of 3-D images by principal direction fields. Graphic models can represent the behavior of fingerprint curvatures [14]. The corner and dominant points are the most important features on curvatures [53] [74]. Qinghan [77] [78] used feature lines to identify fingerprints. Although fingerprints seem to be composed of curvatures, the dominant points of fingerprints are not so unique that they can be considered as reference points.

A pyramidal model was proposed by Hung and Huang [43] which can detect the singular points into a very precise position within 2×2 pixel areas and classify them as core or delta types by the pattern domain of singular points. Hung and Huang [40] also presented a pure mathematical method to find the center of convergence, and a gray zone model to detect the singular points [41].

1.3.2 The Minutiae

Minutiae are randomly distributed in a fingerprint, as shown in Figure 1.1. Minutiae can be considered ridge bifurcations, ridge endings, islands, dots and short ridges. Ratha [83] used an orientation flow field to extract the minutiae. Hung [39] and Pernus [76] modeled the minutiae for fingerprint matching. Hrechak [36] and Maio [62] [64] used structural approach to fingerprint classification by minutiae matching. The process of minutiae matching is like point pattern matching [12] which is slow because of many computations.

Some minutiae are hard to identify because their shapes are smaller and noise sensitive. Among the minutiae, bifurcation is easiest to find. Minutiae cannot be considered

as major reference points when we compare fingerprints because if the printed fingertip is dirty, minutiae are easily removed or added to a fingerprint. It is difficult to find an immutable reference to pattern minutiae other than singular points. Minutiae are useful when singular points are identified and the fingerprint are classified. So, it is understandable that most researchers try to find singular points instead of minutiae [81].

1.4 The Survey of Fingerprint Classification

It is necessary to amplify and catalog fingerprints into more numerous subdivisions. Then we can identity a fingerprint in a smaller subdivision instead of in the whole database. Singular points are commonly used in the classification process.

1.4.1 Henry's Patterns

The most successful person to classify fingerprints was Sir Edward Richard Henry [34] [35]. He classified fingerprints based on the number of singular points and the relationship between them into three major types: arch, loop and whorl, and divided these types into several sub-categories: 1 - plain arches and tented arches; 2 - ulnar loops and radial loops; 3 - composites, that is, combinations of arches, loops and whorls in the same print; 4 - central pocket loops and lateral pocket loops; 5 - twinned loops; and 6 - accidentals which are irregular in outline and can not be placed under central pockets loops, lateral pockets loops or twinned loops. Some samples of Henry's categories are shown in Figure 1.2.

Today Henry's system forms the basis of the great majority of systems employed in English-speaking countries [4]. The organization which has the earliest and biggest fingerprint database in the world is the Federal Bureau of Investigation (FBI) of the United States (US) [20] [92] [93]. Two U.S. institutions, the FBI [21] [22] [23] and the National Institute of Standards and Technology (NIST) [9] [104] [108]. have similar classifications based on Henry's system. The identification process is to match the

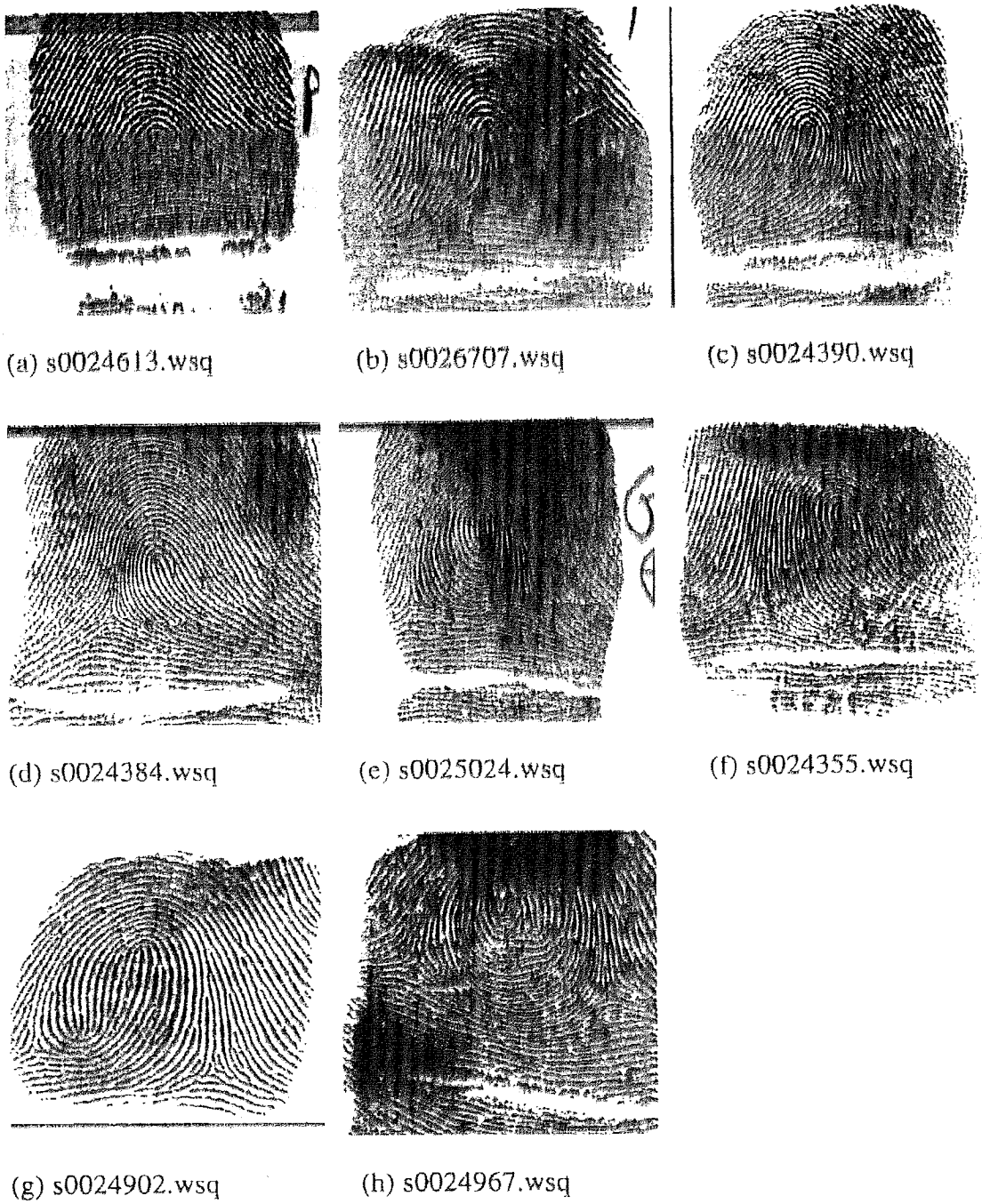

(a) s0024613.wsq (b) s0026707.wsq (c) s0024390.wsq

(d) s0024384.wsq (e) s0025024.wsq (f) s0024355.wsq

(g) s0024902.wsq (h) s0024967.wsq

Figure 1.2 Henry's classification. Arch - (a) Plain Arch. (b) Tented Arch. Loop - (c) Ulnar. (d) Radial. Whorl - (e) Composites - (f) Central Pocket Loop. (g) Twinned Loop. (h) Accidental.

required fingerprint in certain classified groups by minutiae with providing other information such as the ridge counting between singular points [61] [63].

Researchers classified fingerprints to the categories which are similar to Henry's, Cowger [16], Fitz and Green [26], Karu and Jain [49], Kawagoe and Tojo [51], Lin [59] [60], Mehtre [68], Rao and Balck [79], and Wegstein [106]. The classification of Henry's system was pattern-oriented and the correctness is based on visual justification so that it is very hard to distinguish some similar types of fingerprints. Therefore, precision and correctness is reduced and the time for identification is increased.

A new representation model, *Fault Line Graph (FLAG)* which is a bipartite graph [65], was proposed by Hung and Huang [37] that fingerprints can be described by the geometrical relationships between singular points and fault lines which are the boundaries between two different *directional regions*. By this method, fingerprints can be normalized into a fixed orientation by the *horizon vector* in the *FLAG* and can be classified into hundreds of thousands of groups.

1.4.2 Syntactic Approach

There is another method, "Syntactic Pattern Recognition", also called "Pattern Description Language", which presents patterns in terms of grammar rules to produce expressions. Fu [27] [28] [29] [69] first introduced this technique. He used a formal language technique to describe the patterns. Denning [17], Gonzalez [31] and Sudkamp [96] addressed the fundamental concept of languages and grammars. Rao and Balck [82] proposed a syntactic approach to classify fingerprints. They used strings of symbols to represent the curvature of the fingerprint. Moayer and Fu [71] demonstrated a tree system to represent and classify fingerprint patterns. They used a regular tree language to describe the patterns. Lee [56] used tree automata in pattern recognition. Xiao [109] post-processed the fingerprint by combining the statistical and structural method [36]. Hung and Huang [42] proposed a syntactic structure method to represent an object.

The syntactic method is seldom applied to fingerprint research nowadays because it is too complicated to test. In addition, it is highly dependent on human processing. However, the syntactic method is useful in representing and comparing patterns when the patterns have been itemized; that is, after the singular points have been detected and classified. In fingerprints, the directional method is more widely used than the syntactic method [70] [82].

1.5 The Analytical Study on Fingerprint Recognition

Here, we show our fingerprint architecture for the detection of singular points and the classification of fingerprints in Figure 1.3. For each phase of our architecture is explained by following:

a) Fingerprint Imprint: Whether fingerprint is acquired from actively or passively, it should be transferred into a gray scale digitized image.

b) Segmentation and Direction Computation: First, we extract only the fingerprint images with fixed size from the bigger digitized fingerprint cards. The segmentation process will threshold the images into two levels which we call ridges, valleys and backgrounds [38]. Since fingerprints are flow-oriented, we can compute pixel-wise direction by our fuzzy template technique.

c) Singular Points Detection: As previously stated, the singular points are the global patterns in fingerprints. The detection of their accurate position is one of the major topics in our dissertation. The pyramidal model can detect singular points within a 2×2 pixel area.

d) Fingerprint Normalization: Representing fingerprints by Fault Line Graph (*FLAG*), we normalize each fingerprint into fixed orientation by their core-delta pair vector.

e) Fingerprint Classification by the *FLAG*: Using the attributes of core-delta pair vector in (*FLAG*), we can classify fingerprints into millions of groups by mathematical

methods where each group contains only a few fingerprints. If the fingerprints are in the same group, the final minutiae matching will be applied to do each individual fingerprint. So, the time of identification can be reduced significantly.

1.6 The Outline of this Dissertation

The outline of this dissertation is organized as follows.

Chapter 2: Direction computation and analysis.

Chapter 3: Singular points detection.

Chapter 4: The fault line graphs and their normalization.

Chapter 5: The Multi-Index model for fingerprint classification.

Chapter 6: Conclusion

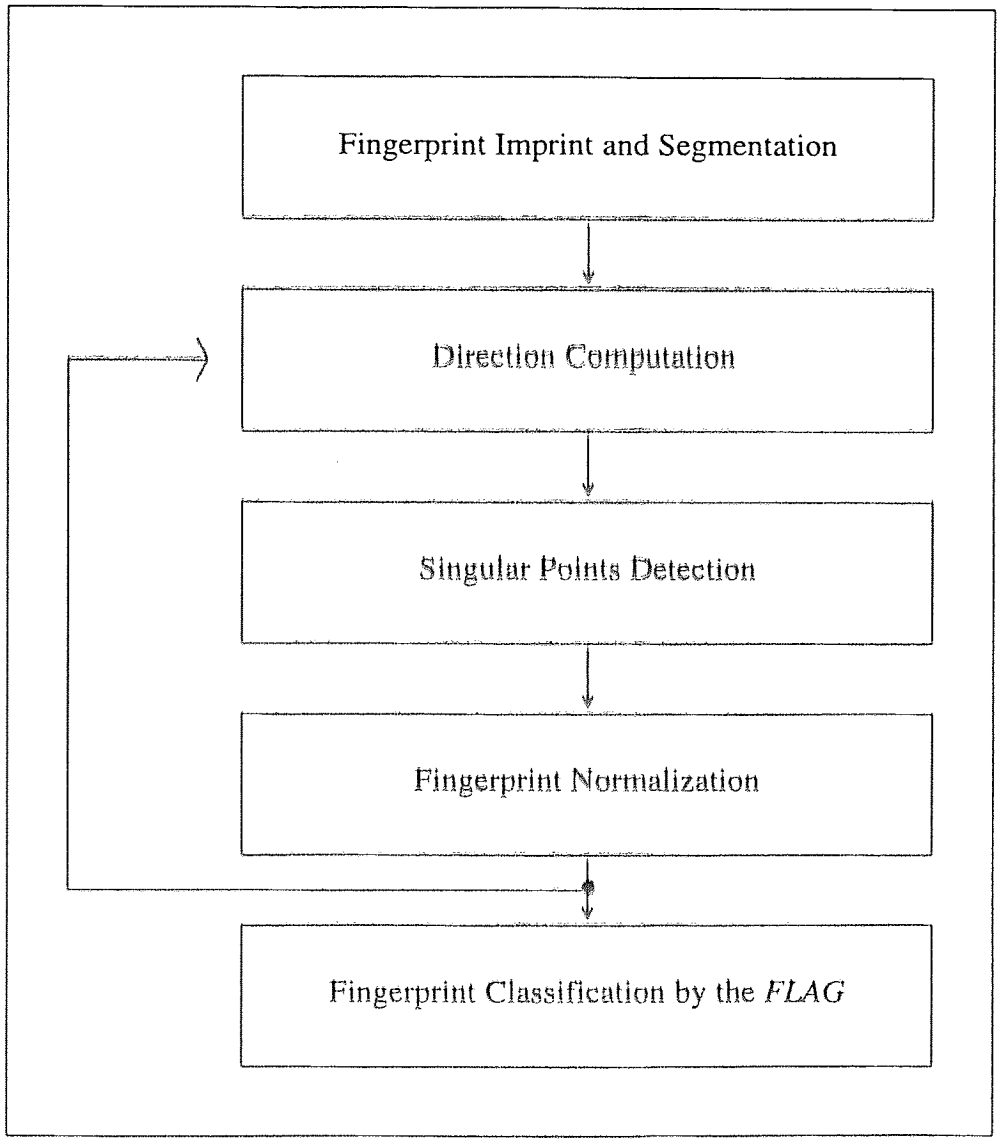

Figure 1.3 The analysis, classification and recognition of fingerprints.

CHAPTER 2

DIRECTION COMPUTATION AND ANALYSIS

It is a well-known fact that fingerprints are flow- and direction-oriented images. Thus, the directional techniques are commonly applied to compute the directions of ridges and valleys, which the resulting images are called *directional images*. The directional images are helpful in analyzing and detecting features of fingerprints. In this chapter, we propose a fuzzy model to improve the speed and compute better pixel-wise directional images of flow oriented patterns such as fingerprints. A fuzzy template can be balanced with any directional number N and size W so that the noise can be reduced. We also prove the best number N for directional images is 3.

2.1 Direction Computing

After thresholding of the fingerprint image, a fingerprint is represented as black ridges, white valleys and background fields. The fingerprints have singular points as global patterns and minutiae as local patterns, respectively. A flow image can be described as a set of concentric ridge flows. As well known, ridge flows are a direction-oriented characteristic. Image quantization is a standard image processing procedure for converting a continuous numerical scale into a finite number of levels by discrete directions. Given a uniformly-distributed quantization, the smallest quantization error is half the size of a converting step. Thus, the direction field of a fingerprint will be quantized into a number of uniformly-valued regions which are locally merged at the singular points. The direction number is ranged from 0 to N-1 if N directions are applied to the image.

Let N be the number used in representing directions of ridge flows and $D = \left\{ d_1, ..., d_N \right\}$ be a set of integer directions which represent directional orientation

ranging (0, π]. A pixel's P_{ij} direction is determined by computing all connected pixels of neighbors Q_{ij} which are the same type (ridge or valley) as P_{ij} within WxW area. Then the maximum one in the direction histogram is assigned as P_{ij}'s direction.

2.1.1 Pixel-wise Calculation

Let $W = 2w+1$, for each pixel $P_{ij} = (i,j)$, a $W \times W$ domain centered at p is used and the domain is denoted as $\Omega_W(P)$. Given $q = (a,b) \in \Omega_W(P)$, the N orientation of a line linking of P and q is defined by

$$d_n(P,q) = \begin{cases} Quan\left[\tan^{-1}\left[\dfrac{b-j}{a-i} \right] \right] & , \text{ if } q \text{ is connected to } P, \\ -1 & , \text{ otherwise.} \end{cases}$$

where -1 marks a status of invalid and *Quan* is a quantization function which the resulted value is in { 0, 1, ..., N–1 }. Then the local direction $d(P)$ is set to the majority direction over the domain of $\Omega_W(P)$. If no majority direction can be found or multiple directions are found having similar high counts, a higher domain of $\Omega_{2W}(P)$ is applied. If a majority still can not be found, then $d(P)$ is set to -1 or a status of invalid. The direction of a ridge line can be also consider as its slope.

2.1.2 Fuzzy Circular Technique

After thresholding the gray scale image, the image is cataloged into 2 distinct levels; ridge and valley. In a square region, the distance to border of the square in the diagonal direction is larger than the distance to the vertical and horizontal directions. We propose a circular method to compute the direction because the circle has a balanced number for every direction. A circle is first divided into $2N$ directions, in which each cone contains π/N angle. Then it is applied on a digitized grid plan with a radius w. ${}_{ij}C_{mn}$ is the pixel at P_{mn} within the circle on the digitized area as center at (i,j).

In Figure 2.1, we can find that there are some pixels which are right on the directions 0, 1 and 2, but most pixels are not (shown as the marked area). It is no doubt that these pixels on the direction 0, 1 and 2 should have that direction. But most of them are uncertain. Then, the fuzzy concept is allied to solve this problem. For any pixel $P_{mn} \in \{_{ij}C_{mn}\}$ satisfying the following fuzzy equation is called an actual pixel. $\{_{d}V_{ij}\}$ is defined as the fuzzy type marker of direction of P_{ij}:

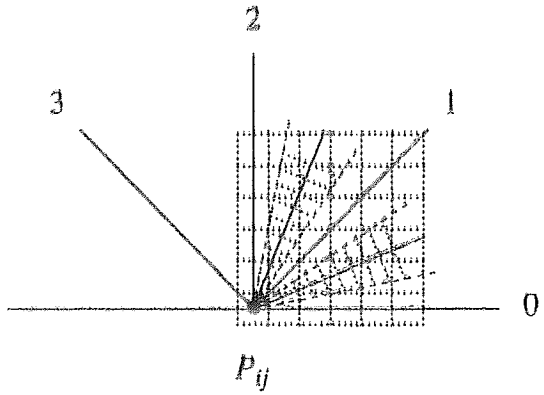

Figure 2.1 The Fuzzy quadric region when $N = 4$.

$$\frac{\pi}{4N} * (k-1) \le f(i,j,m,n) \le \frac{\pi}{4N} * (k+1), \quad \text{for } k = 0, 4, \ldots, 4(N-1)$$

where $f(i,j,m,n)=sin^{-1}(\frac{(m-i)}{\sqrt{(i-m)^2+(j-n)^2}})$ The $\{_{a}V_{ij}\}$ of actual pixel $\in$ { 0, 1, 2, ..., $N-1$ }. And, for any pixel $P_{mn} \in \{_{ij}C_{mn}\}$ satisfying the following fuzzy function is called a uncertain pixel.

$$\frac{\pi}{4N} * (k-1) \le f(i,j,m,n) \le \frac{\pi}{4N} * (k+1), \quad \text{for } k = 2, 6, \ldots, 4(N-1)+2$$

The uncertain pixel's $\{_{z}V_{ij}\} \in \{ \{0, 1\}, \{0, 2\} \ldots, \{0, 1, \ldots, N\text{-}1\} \}$ which is a fuzzy set. So, we have the fuzzy direction marker of P_{ij} when $N = 3$ direction as following:

$$_{d}V_{ij} = {}_{a}V_{ij} \cup {}_{z}Q_{ij} = \{ A,B,C,D,E,F,G \}$$

where $A = \{ 0 \}$, $B = \{ 1 \}$, $C = \{ 2 \}$, $D = \{ 0, 1 \}$, $E = \{ 1, 2 \}$, $F = \{ 0, 2 \}$ and $G = \{ 0, 1, 2 \}$. G usually can be ignored. Then we have a fuzzy template T for the image. For each ridge or valley pixel direction D_{ij} computing, the following equation is used:

$$D_{ij} = \max_{d=0}^{N-1} \left\{ \left| {}_{d}V_{ij} \right| \right\},$$

Two templates are shown in Figure 2.2, each of them is centered at the computing pixel by mapping the direction number sets and the template symbols, with $W = 11$ (a) $N = 3$ and (b) $N = 4$. We can see that the pixels marked in sets are those bidirectional areas which are not clearly defined in the most current researches. Given a partial ridge flow as Figure 2.3(a) which the center is located at P_{ij} marked as "●" and the region within $W \times W$ is enclosed by a square, the valid 8-connected neighbors for computing P_{ij}'s direction are marked as "+" after the template is applied, as shown in figure 2.3(b). Figure 2.3(c) shows the results with $W = 11$ and $N = 3$. Direction d_0 has 7 pixels, direction d_1 has 16 pixels and direction d_2 has 22 pixels. Direction d_2 is assigned to P_{ij} because it has the largest weight.

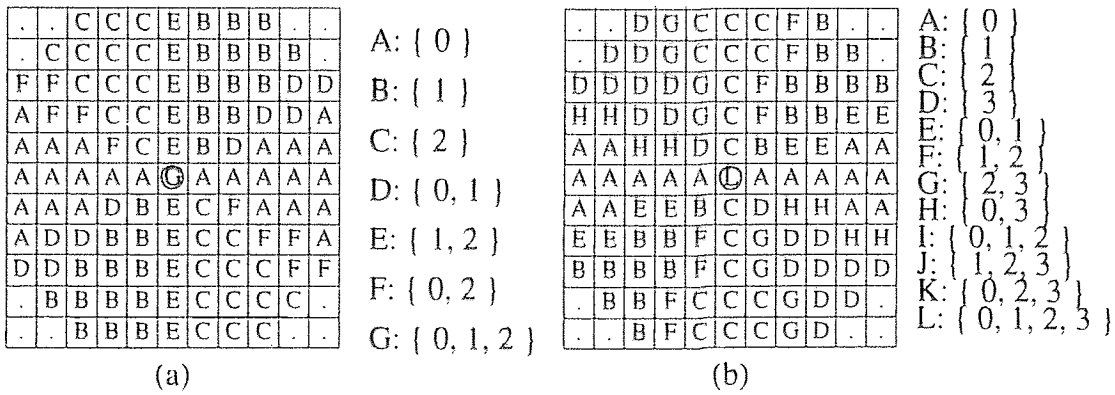

Figure 2.2 Template by mapping symbols and direction sets, with $W = 11$ (a) $N = 3$ and (b) $N = 4$.

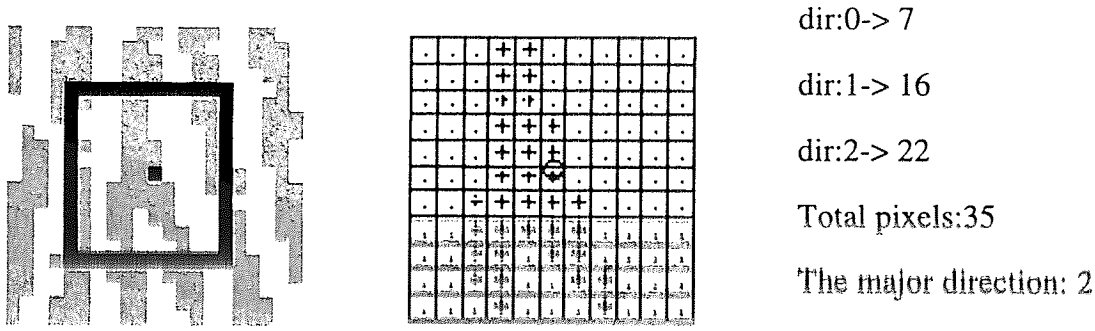

Figure 2.3 (a) The ridge flows, (b) the mask with "o" indicated as pixel P_{ij} to be tested, (c) the result after applied circular template.

Lemma 2.1 The best number N of a fingerprint directional image is 3.

Proof

Given grids of pixels in Figure 2.4(a) with N direction and $W = 2w + 1$ where w is the distance from center pixel to its 8-connected neighbors, each direction angle δ is π/N and the angle ϕ between two contiguous pixels under same w is $2sin^{-1}(1/2w)$, shown in (b). When we inspect two fault lines merging area which is 3×3 pixels and $w = 1$, ϕ will be $2sin^{-1}(0.5) = 60^o$.

Let $\delta = \phi$, then N will be 3.

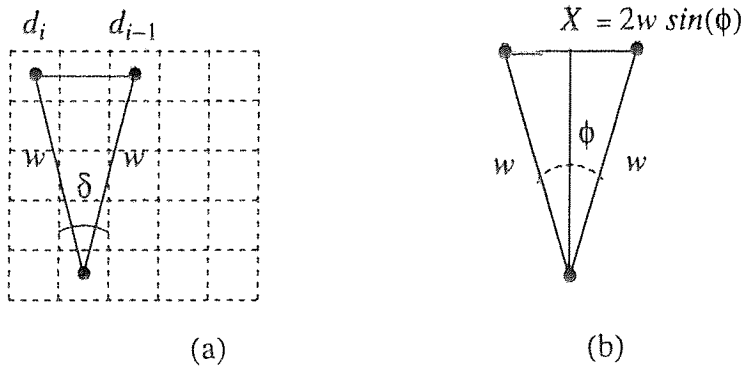

Figure 2.4 (a) N directions (b) the angle ϕ between two continuous pixels.

2.1.3 Smoothing

After the directional image is computed, it is necessary to smooth the image to filter the local disturbance. Let $S(w,h)$ be a smoothing function which returns the direction with h% frequency in $\Omega_W(P)$. For example, given a partial ridge in Figure 2.5(a), there are some noises in the directional image as shown in Figure 2.5(b). The resulting image after smoothing by using $S(5,0)$ is shown in Figure 2.5(c).

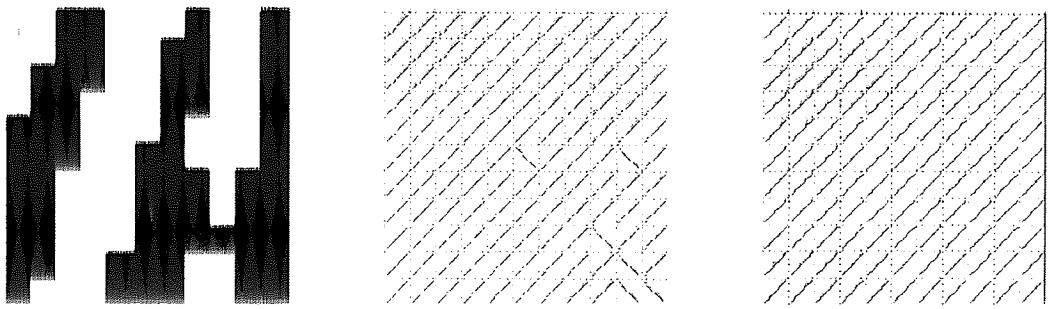

(a) (b) (c)

Figure 2.5 The smoothing procedure. (a) The given ridge flows. (b) is the pixel-wise directional image. (c) is the smoothed directional image of (b). "__", "/" and "\" represent the direction 0, 1 and 2, respectively.

2.2 Experiments and Results Analysis

By our experiments, The average width of ridges and valleys is around 7.4 pixels under 500 dpi resolution. The template size needs to be bigger than the average width. In our experiments, we use $W = 11$. It is noticed that the direction-crossings of a digitized directional image are convergent toward a point. In practice, direction-crossings will merge before they reach the prospect point; that is, a phenomena of a premature convergence.

To explain the fundamental fingerprint process which includes the segmentation and direction computation, we use two fingerprints in Figure 2.6(a) and (b) for the demonstration. After applying the fingerprint extraction and segmentation (please see the Appendix A and B), the thresholding images are shown in Figure 2.6(c) and (d). The smoothed directional images are shown in Figure 2.6(e) and Figure 2.6(f), respectively.

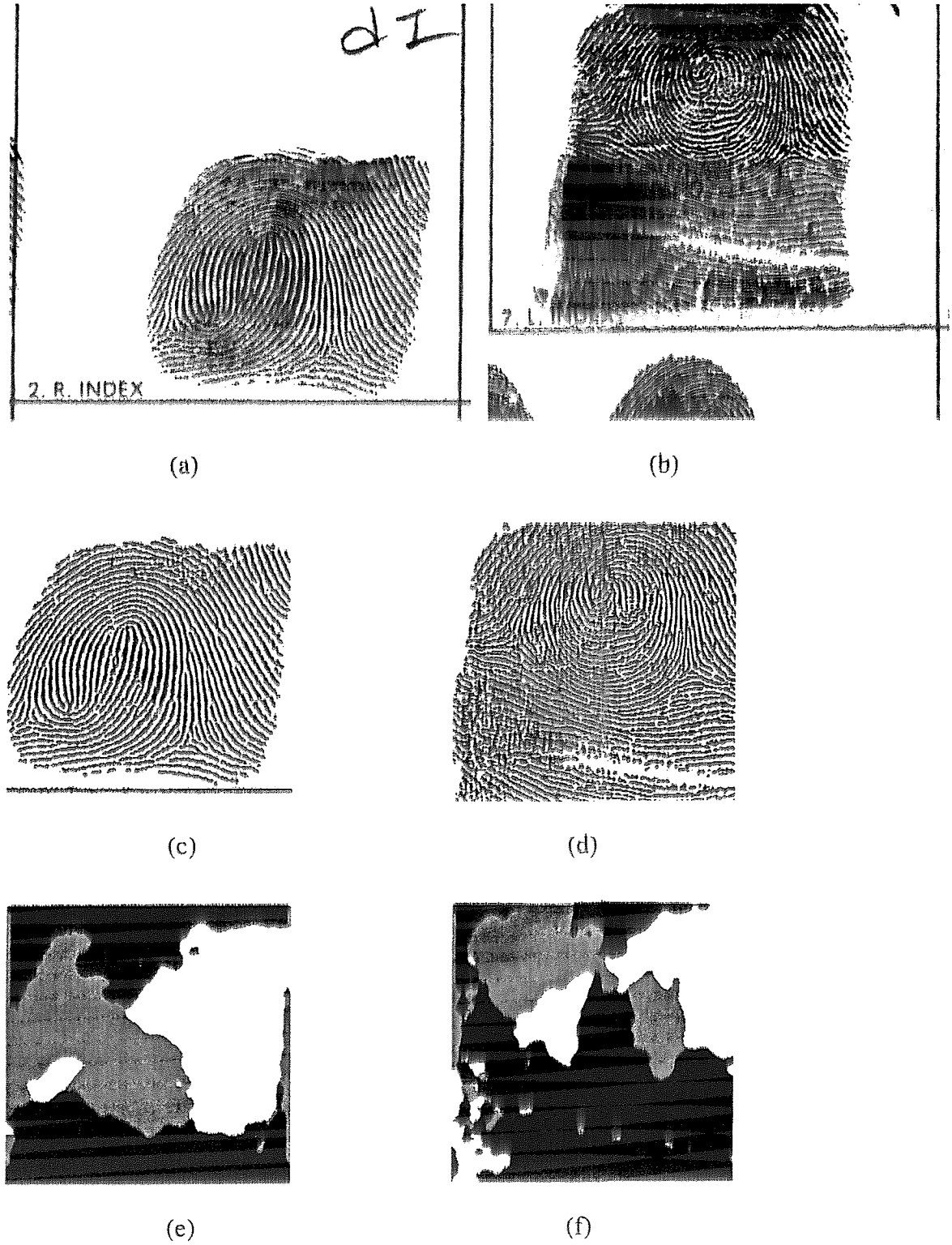

Figure 2.6 The more experimented result from test database. (a) s0024902.wsq (b) s0024967.wsq. (c) is the thresholded result of (a). (d) is the thresholded result of (b). (e) is the directional image of (c). (f) is the directional image of (d).

Using a fingerprint s0024384.wsq from the NIST image database as a sample shown in Figure 2.7(a), we compute its direction image by applying the template under different N as 2, 3, 4, 6, 8 and $W = 11$. The results are shown in (b), (c), (d), (e) and (f), respectively. It is clear that when $N = 3$ a better directional image is achieved. If N is bigger, there will be a premature phenomena of fault lines. If N is less then 3, the directional image features are lost. To reduce the aforementioned phenomena, obtained directions are quantized into 3 orientations in most of the experiment results. If N is not 3, we will specify the number.

2.3 Definitions and Characteristics of Directional Images

According to the features of directional images, we define several related terms which will be used later and induce the characteristics based on the definitions.

2.3.1 Definitions

- A *directional region* $\Omega(i)$ is colored by number i if the majority of the pixel-wise directions is d_i within the closed region.
- A *fault line* ψ_k is defined as the boundary between two different directional regions $\Omega(i)$ and $\Omega(j)$ with $k = i + j$, $d_i \neq d_j$ and $d_i, d_j \in \{0, 1, ..., , N\text{-}1\}$; denoted as $\psi_k = \Omega(d_i, d_j)$.
- A *virtual fault line* ψ_k' is assumed to connect disconnected segments of a fault line, ${}_a\psi_k$ and ${}_b\psi_k$, causing by a broken fault line ψ_k because of reaching the image borders or noises. We still consider ${}_a\psi_k$, ψ_k' and ${}_b\psi_k$ to be one fault line ψ_k. As shown in Figure 2.8, the fault line ψ_1 is combined by ${}_a\psi_1$, ψ_1' and ${}_b\psi_1$, and the fault line ψ_2 is combined by ${}_a\psi_1$, ψ_2' and ${}_b\psi_2$. We will discuss why the fault line ψ_1 is not combined by ${}_a\psi_1$ and ${}_b\psi_2$ later.

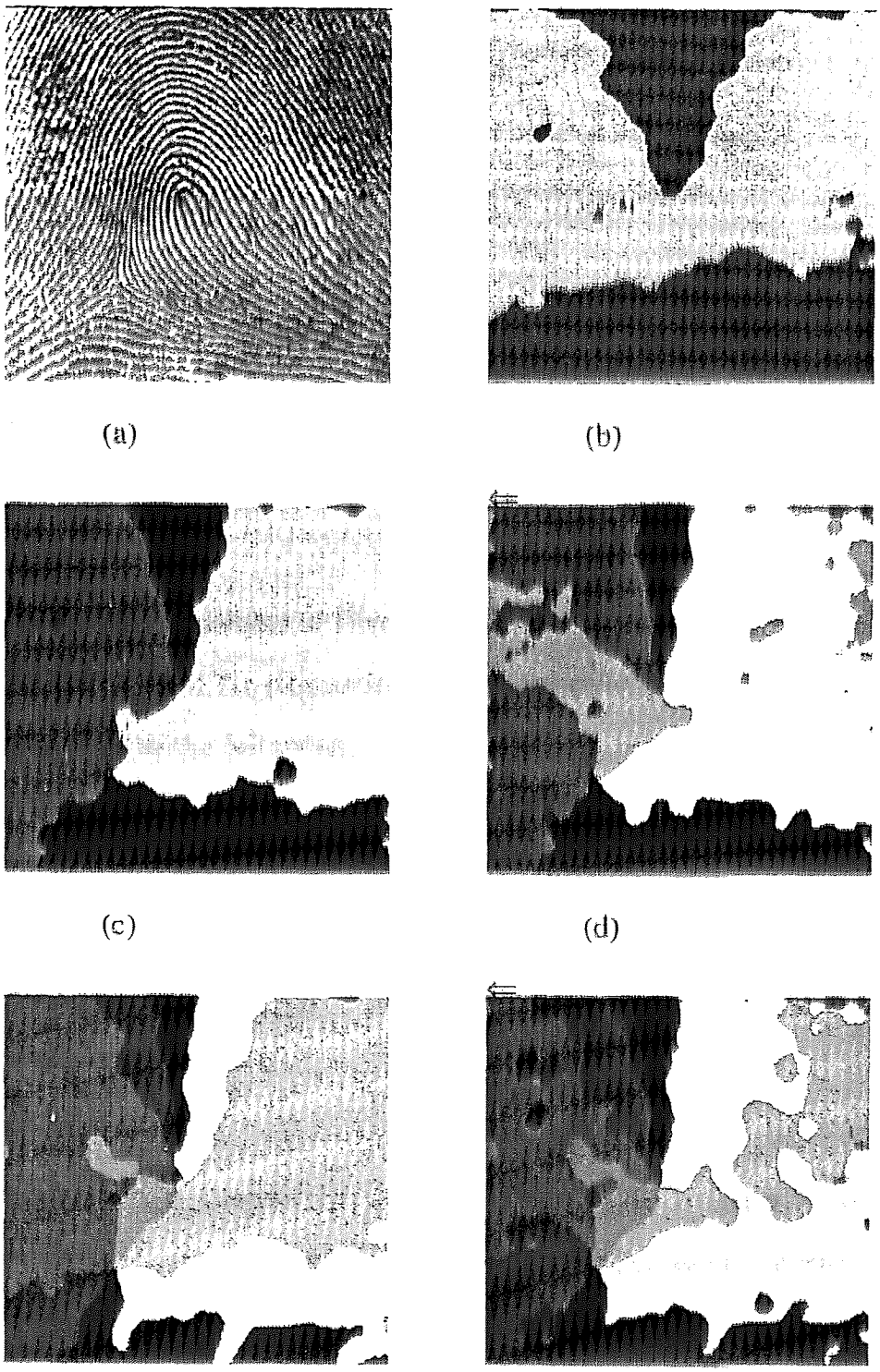

Figure 2.7 (a) The original fingerprint image (b) directional image with $W = 11$ and $N = 2$ (c) $N = 3$ (d) $N = 4$ (e) $N = 6$ (f) $N = 8$.

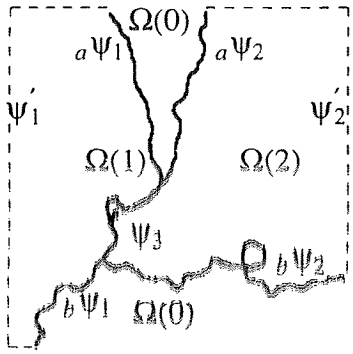

Figure 2.8 The fault lines representation of Figure 2.6(c). (a) A fault line ψ_3 is collided by $\Omega(1)$ and $\Omega(2)$. The fault line ψ_1 is combined by ${}_a\psi_1$, ψ_1 and ${}_b\psi_1$ where ψ_1 is a virtual fault line.

2.3.2 Characteristics of Directional Images

We can induce the characteristics of directional images based on the definitions in Section 2.3.1 as the following:

- A physical region is a closed area.
- Based on the aforementioned fact, a directional region is a closed area which has boundary consisting of a sequence of connected fault lines or image borders, as shown in Figure 2.8.

2.4 Conclusions

In this chapter, we proposed a new fuzzy model to get a better pixel-wise directional image. We proved $N = 3$ will result in better directional images. Also, we analyzed the effect of different number of directions. The bigger the number, the more noisy; the smaller, the less information.

CHAPTER 3

SINGULAR POINTS DETECTION

Singular points, cores and deltas, are the most important global patterns of fingerprints in convergence and divergence of ridges, respectively. Computationally, a singular point is defined as a location where a local maximum in ridge curvature is detected. That is, singular points can be analytically extracted as representational directional patterns. The features of singular points can be more easily demonstrated on directional images. In this chapter, we first analyze the characteristic of the directional image and discover the patterns of cores and deltas. Then, a pyramidal model is proposed to detect more precise position of the singular points with better performance. Several experiment results are then shown to explain our methods.

3.1 Definitions and Characteristics of Fault Lines

First we define several terms for fingerprint images and induce the characteristics of fault lines based on the definitions. These terms and characteristics will be used often during this dissertation.

3.1.1 Definitions

- A *singular point* is defined as the location of the maximal direction changing area which contains all N directions. From chapter 2, we know there will be a fault line if there is a direction changes. In other words, a singular point is the intersection area of fault lines. Since $N = 3$ is used, a singular point should contain 3 directions $\{0, 1, 2\}$. The singular points can be classified into two types: cores and deltas.

- Topologically, directional measurements obtained along a circular trajectory surrounding a *core* are monotonically varying from 0 to 2π.
- Different from a *core*, the direction changes around a *delta* can be divided into 3 disconnected ranges, each of which is monotonically decreasing.
- A *directed fault line* is a fault line with a direction.
- An *out-going fault line* is a fault line pointing from the higher curvature ridge region to the lower curvature area as shown in Figure 3.1(a).
- An *in-going fault line* is a fault line pointing from the lower curvature ridge region to the higher curvature area.
- A *connection* is defined between two singular points through fault lines.
- A *direct connection* between singular points is established through only one fault line ψ_k without transitive by other singular points.
- A *indirect connection* is defined as two singular points which are not directly connected, but they are connected via other singular points transitively.

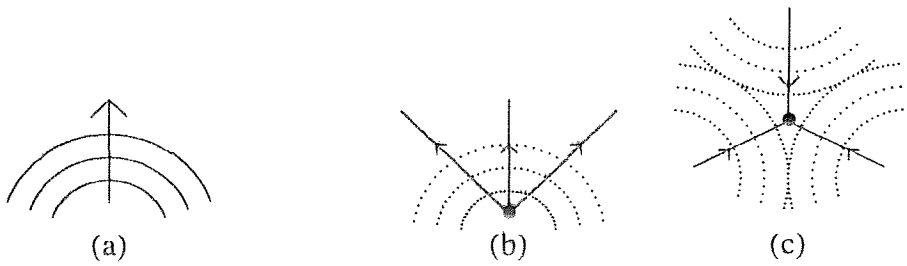

Figure 3.1 The Directed fault lines. (a) shows a directed fault line from higher to lower curvatures. (b) shows a core is the joining point of out-going fault lines. (c) shows a delta is the joining point of in-going fault lines.

3.1.2 Characteristics of Fault lines

- A singular point is the intersection point of exactly 3 fault lines.
- A core is the intersection point of out-going fault lines as shown in Figure 3.1(b).
- A delta is the intersection point of in-going fault lines as shown in Figure 3.1(c).

- Due to the under-sampling effect of image quantization, the center of an ideal circle can be classified as a core-core singular point pair. (shown as Figure 3.2.)

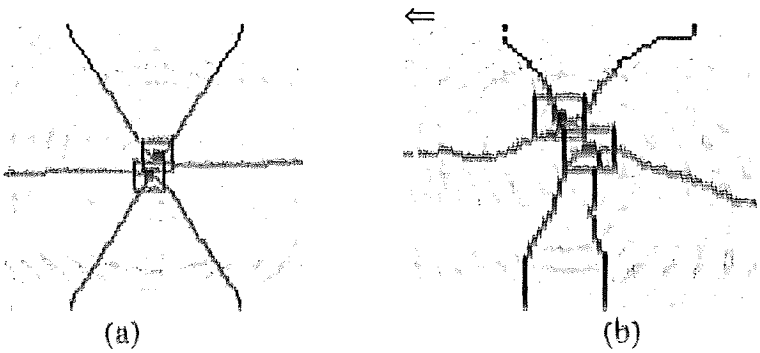

Figure 3.2 A core-core pair has been detected in (a) a set of computer-synthesized concentric circles containing cores, (b) a fingerprint consisting of a whorl pattern.

3.2 The Detection of Singular Points

Since fingerprints are direction-oriented and singular points are global patterns of ridge flows, we can summarize the directional patterns of cores and deltas into certain domains. We can then detect their positions more precisely and efficiently using a multi-layered pyramidal model and classify them as core or delta types. The singular points can be detected in almost pinpoint area of 2×2 pixels which is the only possible smallest size.

3.2.1 The Domains of Singular Points

According to Henry's classification [35], a singular point can be classified as core and delta types. Let $\Omega_s(P)$ be a function containing the pixels' direction within a $s \times s$ pixel area starting from P. By definition, the singular point should be located at a region $\Omega_s(P)$ containing all 3 directions {0, 1, 2} with $s \geq 2$.

Let $u_i(P)$ with i = { 0, 1, 2, 3 } be the members of a 2×2 domain $\Omega_2(P)$ where $u_0(P)$ is located at the left top corner, and $u_1(P)$, $u_2(P)$ and $u_3(P)$ are in clock-wise direction around the 2×2 pixels, as shown in Figure 3.3(a). From the experiments, a core

directional pattern will be "2 → 1 → 0" and a delta directional pattern will be "1 → 2 → 0" in clock-wise manner starting from $u_0(P)$ around the $\Omega_2(P)$. The patterns of cores and deltas are shown in Figure 3.3(b) and (c), respectively.

The directional shifting is then defined as

$$u_i'(P) = (u_i(P) + 1) \bmod 3, \text{ with } i = 0, 1, 2, 3.$$

It means the directional patterns of singular points can be shifted. In other words, a core pattern can be shifted as "1 → 0 → 2" and "0 → 2 → 1", and a delta pattern can be shifted as "2 → 0 → 1" and "0 → 1 → 2".

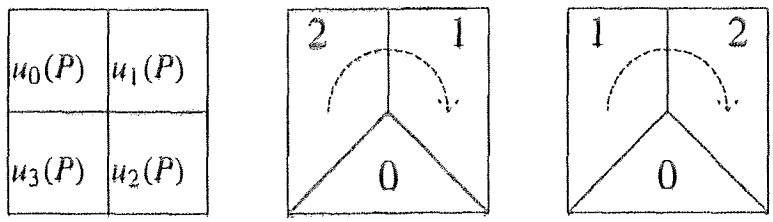

Figure 3.3 (a) defined the directional domain of a singular point in a $\Omega_2(P)$ area. The patterns of a core and a delta points are shown in (b) and (c), respectively.

3.2.2 The Multi-layer Hierarchy

Let $S^f_k(I_k)$ be an operator to an image I which is shrunk or enlarged by a factor of $(r \times r)^k$ where k is the layer number and f is the control variable which could increase or decrease by 1. The new image created by such an operator is called the kth shrinking or expanding layer accordingly. It is denoted as

$$I_k = S^f_k (I_{k+f}), \text{ with } f = 1 \text{ or } -1.$$

where I_0 is the original image. For each pixel, in the domain of I_k, its value is set to the majority direction of the corresponding $r \times r$ sub-image in I_{k-1}. The whole procedure is illustrated in Figure 3.4, to which the shrinking procedure is shown to the left hand side

from lower layer I_0 to higher layer I_n while the searching process is shown in the right hand side from top I_n to bottom I_0. *a) Shrinking Phase*: It is obvious that a pattern in I_{k-1} layer, which is not the majority in $r \times r$ area will disappear from I_k layer. Thus, spurious patterns or local ridge disturbances caused by the formation of minutiae can be totally ignored by performing a proper sequence of shrinking operators. That is, the highest layer I_n of a pyramid of n shrinking layers contains only the characteristics of the major singular points, though its precision is one in $(r \times r)^n$. The new pixel P_{mn} on I_k will be the majority of down layer I_{k-1} which cover the rectangle area $\Omega_r(P_{mn})$.

b) Searching Phase: Starting from the highest shrinking layer I_n, the corresponding sub-layer domain $S_n(\Omega_2(P))$ for each singular point candidate (P, h) has to be examined. First, the precision will be improved from one in $(r \times r)^n$ to its descendant in $(r \times r)^{n-1}$. The type and the orientation of the new-found singular point candidate $(P', h-1)$ must the same as those of the singular point (P, h). Subsequently, each candidate (P', h) in hth layer must have its sub-layer domain examined in order to locate a more precise candidate in $(h-1)$th layer. This procedure continues until the highest precision or the original layer I_0 is reached.

3.2.3 Spurious Candidate Elimination

Theoretically, each candidate in hth layer must have one corresponding candidate in the $(h-1)th$ layer and both of them are the same sub-type. As the resolution increases, however, the number of aforementioned spurious candidates increases. In addition, the sub-type of the one in lower layer may be deformed due to under-sampling effect.

In the searching phase, the sub-type of a found lower-layer candidate must match that of its parent layer. In addition, each member in domain $\Omega_2(P)$ must have enough number of same type, 8-connected neighbors so that the found candidate is not a local

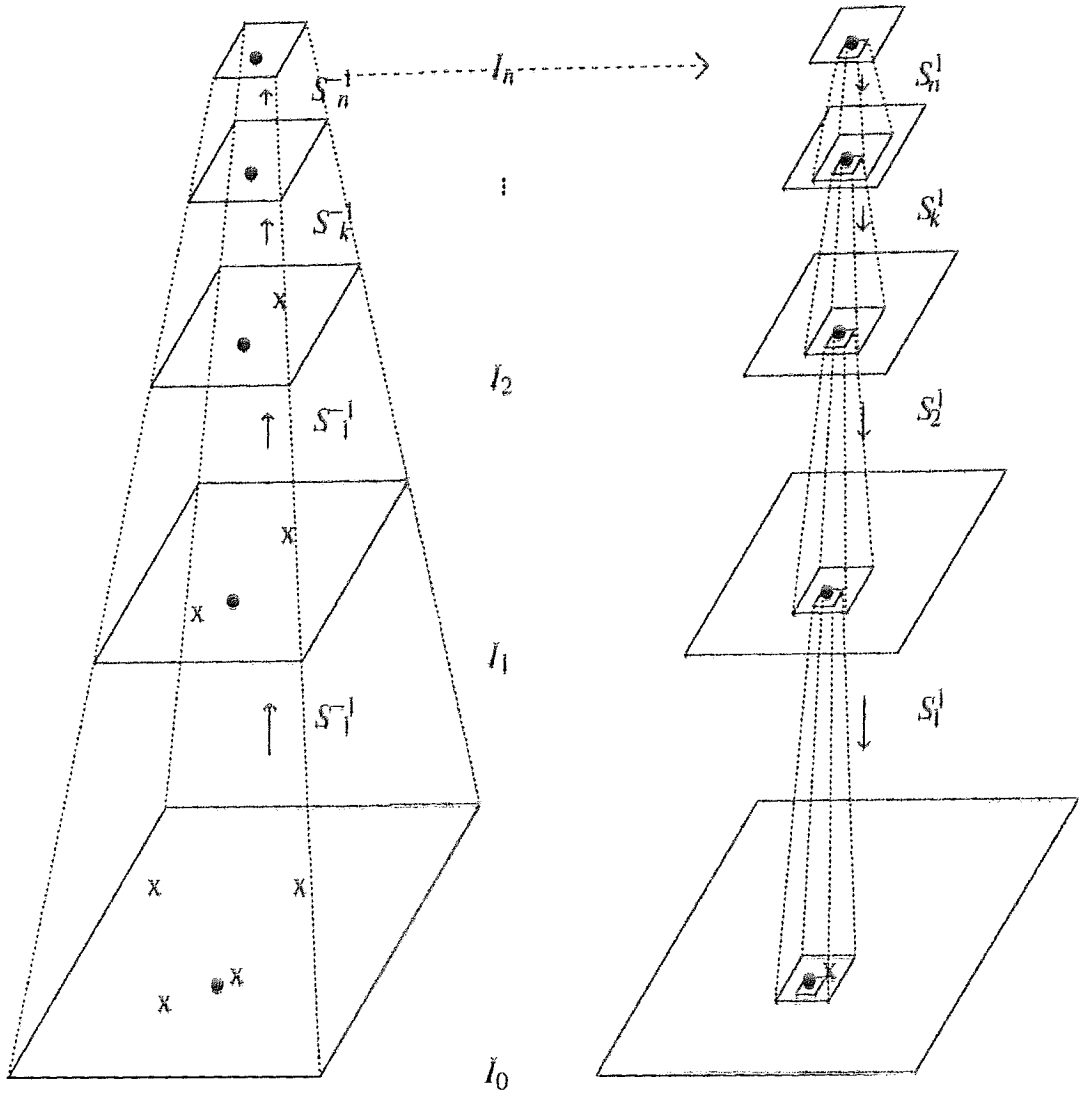

Figure 3.4 Illustration of the proposed pyramidal model where each '•' marks a correct singular point and each 'x' marks a direction anomaly.

disturbance. The number of required neighbors can be defined as $(r \times r)^k$. By this way, we can remove spurious candidates induced by the under-sampling side effect and noise.

Each sequentially searched square sub area in different layers has the same size. When a candidate is detected within a 2×2 window during the searching process, the effective searching area is enlarged to $2r \times 2r$ in a lower-layer. The same procedure is recursively applied until the lowest layer is reached. The final singular points are detected on the bottom layer and the size of each one is only 2×2 pixels.

Under the consequence of the digitizing process, a point will shift around a half pixel to its neighbors. That is the reason why we can not claim that the singular points are detected in pinpoint size of 1×1 pixel.

3.3 The Theorems

After the fault lines and singular points are detected and classified, we can induce some theorems based on their characteristics as follows:

Theorem 3.1 Fault lines only intersect at singular points, if the direction number $N = 3$.

Proof

Let ψ_i and ψ_j be fault lines with $\psi_i = \Omega(D_a, D_b)$ and $\psi_j = \Omega(D_c, D_d)$. Assume that ψ_i intersects with ψ_j at a point $P = (x, y)$ where P is not a singular point and $\psi_i \neq \psi_j$. Since we use 3 directions, $D_a \cup D_b \cup D_c \cup D_d = \{D_0, D_1, D_2\}$. That means the area $\Omega_2(P)$ contains all 3 directions. By definition, this intersection area centered at P is a maximal direction changing area which contains all 3 directions. That means P is a singular point. This contradicts to our assumption. Therefore, fault lines only intersect at singular points.

Theoretically, the fault lines should only intersect at singular points no matter how big the directional number N is. But because of the digitized problem, the fault lines may

be merged before reaching the singular points. We call this a premature phenomenon. To reduce this premature phenomenon we use $N = 3$.

Theorem 3.2 No fault line can be established between two singular points having an identical type.

Proof

From the section 3.1.2, a core point is the joining point of out-going fault lines and a delta point is the joining point of in-going fault lines. Assume that a core point directly connects with another core point, that is, the out-going connects with out-going. If two out-going lines reached from different sides, there would exist a joint point. At this joint point, the flows becomes in-going. According to the definition, the joint point should be a delta point. It contradicts with our assumption. So, two core points cannot directly connect. The same proof can be applied to delta points. So, there cannot be direct connections between same types of singular points.

In other words, the two ends of a fault line must be different type of singular points. That is the reason why the fault line ψ_1 is combined by ${}_b\psi_1$, ${}_b\psi_1$ and ψ'_1, but not combined by ${}_a\psi_1$ and ${}_a\psi_2$ in section 2.3.1.

3.4 Experiments and Results Analysis

An ellipse type fingerprint shown as Figure 3.5 is used to demonstrate our method. On the top of the left hand side is the directional image, and on the top of the right hand side is the original fingerprint. Under the shrinking or searching phases, the directional image is shrunk or expanded by a factor of (3×3). The shrinking phase is shown on the left side of Figure 3.5, while the searching phase is shown on right hand side. The detected singular points under different resolutions are marked as rectangles in each domain and their size indicates the precision.

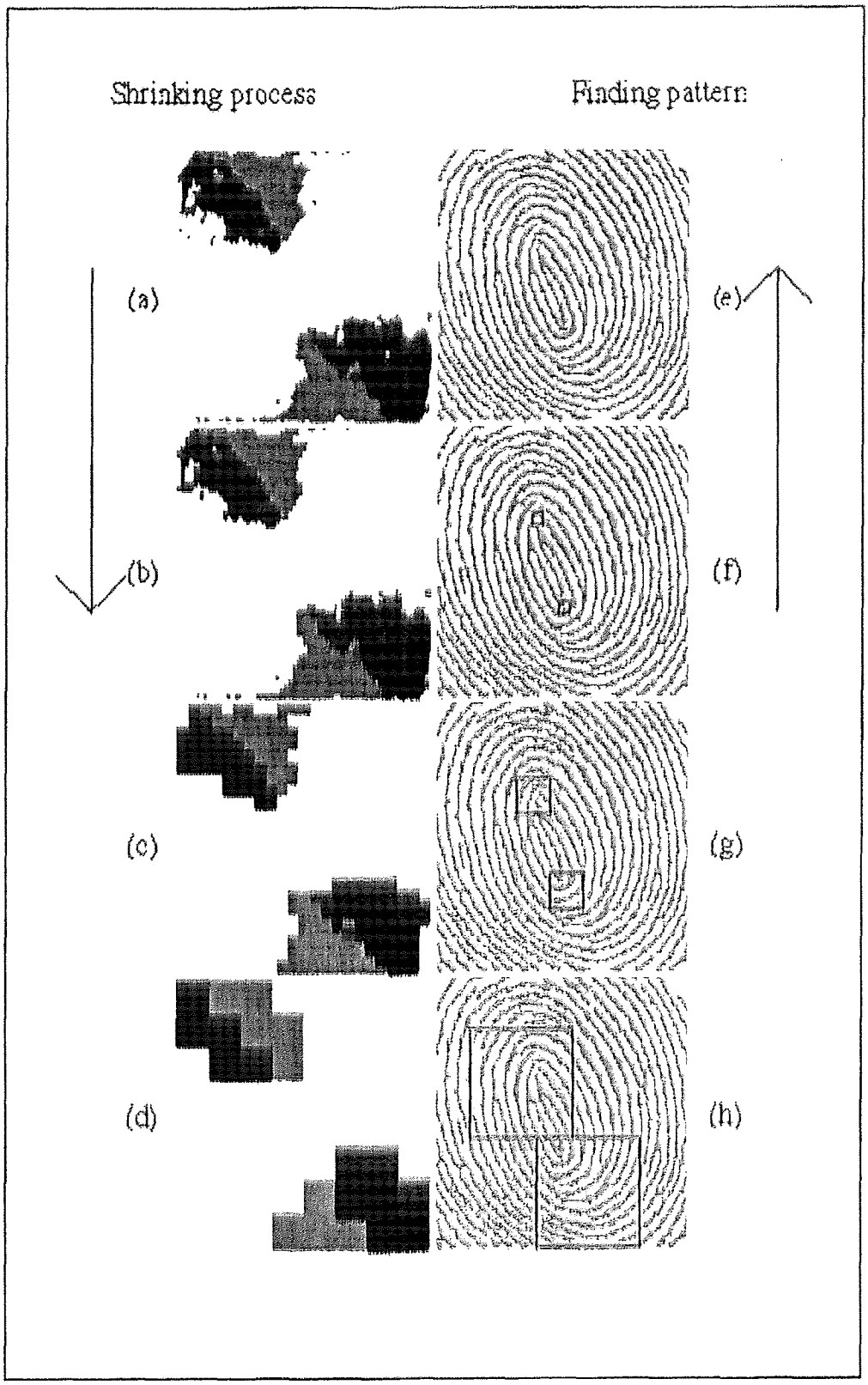

Figure 3.5 The shrinking procedure is illustrated from (a)-(d), while the extracting of singular points are shown upside down from (e)-(h).

(a) s0024613.wsq (b) s0024356.wsq (c) s0024390.wsq

(d) s0024591.wsq (e) s0024386.wsq (f) s0026382.wsq

(g) s0024967.wsq

Figure 3.6 The experimented results with different types of fingerprints from (a) to (g). The squares are shrinking into final detected position with 2×2 pixels.

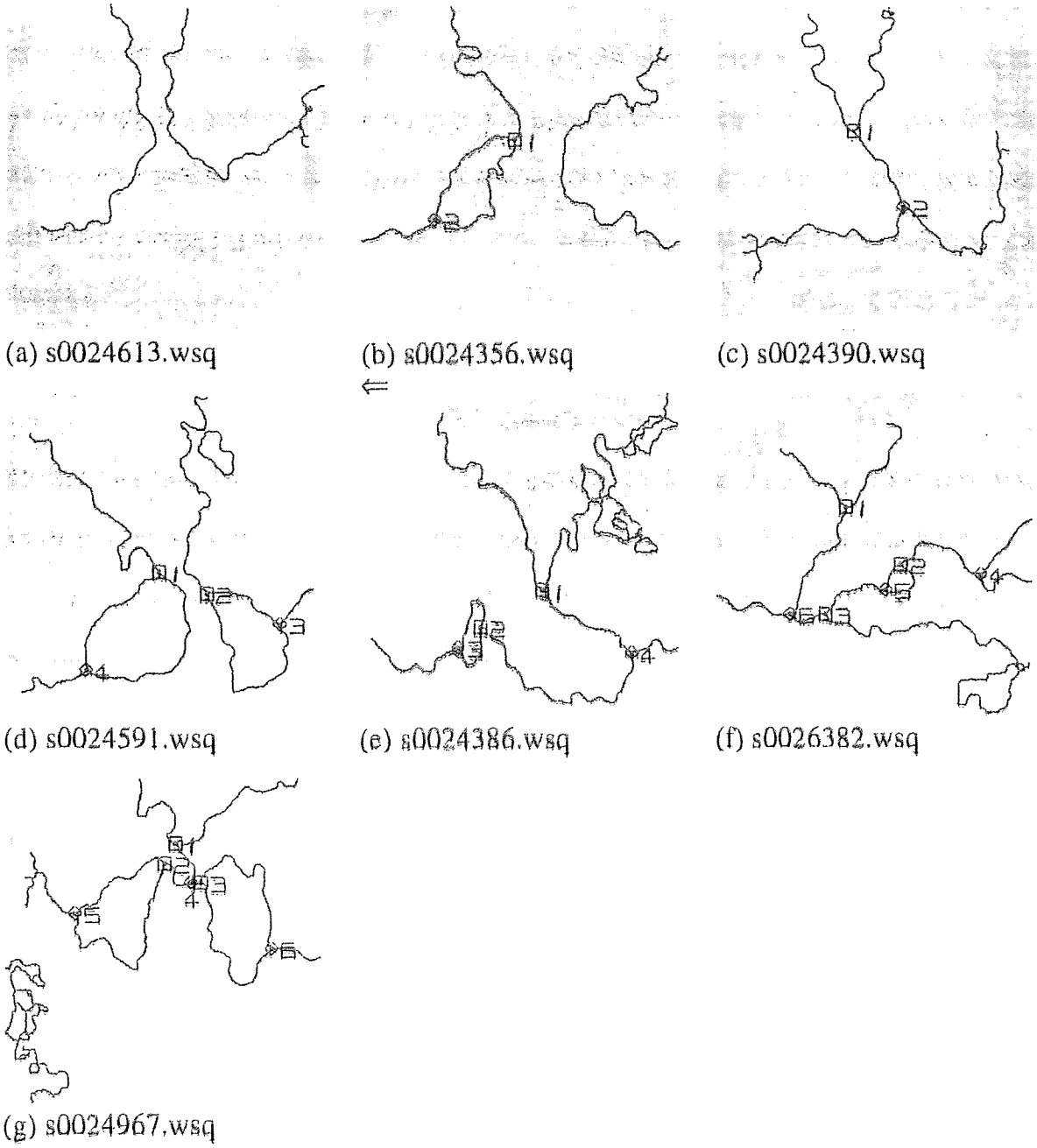

(a) s0024613.wsq (b) s0024356.wsq (c) s0024390.wsq

(d) s0024591.wsq (e) s0024386.wsq (f) s0026382.wsq

(g) s0024967.wsq

Figure 3.7 The classified singular points of Figure 3.6 with marked cores as squares and deltas as rhombuses and connected with fault lines. The numbers indicate the detected order with cores first and deltas later.

The overall methodology is analogous to as operating a telescope. First, we wide search the open space, then gradually adjust the view-finder into smaller regions, finally focusing in on the target. More examples are shown in Figure 3.6. The rectangles in each image are gradually focused onto the singular points, and the final size is 2×2 pixels which are marked as dots. Figure 3.7 shows that the combinations of fault lines and the classified singular points of Figure 3.6 with marked cores as squares and deltas as rhombuses.

3.5 Conclusions

In this chapter, we proposed a pyramidal method to detect singular points from fingerprint images with better accuracy than other similar methods. We can classify them into core or delta type at the time of detection using simple domains. Like a bipartite graph, singular points cannot directly connect to the same type through the fault lines. The experimented results show that our algorithms can precisely obtain singular points within 2×2 pixel areas and classify the detected singular points into cores or deltas. With more precise detection, we can classify fingerprints into more categories and reduce the time of matching processes.

CHAPTER 4

THE FAULT-LINE-ANALYSIS-GRAPHS AND THEIR NORMALIZATION

In this chapter, a fingerprint by a *fault-Line-Analysis-Graph (FLAG)* with singular points as vertices and fault lines as edges. We propose and prove some theorems that singular points must exist in core-delta pairs and the *FLAG* is a perfect matching. A pattern model is also proposed to analyze and predict the location of singular points. Then, a computational method can transform fingerprints into invariant orientation by the *reference vector* formed by the singular points. When a fingerprint is processed, it can be in any orientation. How to transform the fingerprints into same orientation is very important to further classification. The current classification or comparison methods mostly assumed fingerprints were oriented acceptable, which could be done manually. However, manual adjustment reduces the efficiency and precision of classification and may cause incorrect identification.

4.1 The Fault Lines Graphs (*FLAG*)

Let a graph $G(C, D, E)$ represent a fingerprint as C and D are the vertices set of core and delta points, respectively, and E is the edge set of fault lines. The singular points will be adjacent to each other through fault lines. Using Figure 3.7 as the example, the singular points, cores marked as "o" and deltas marked as "◉", the new represented *FLAG* are shown in Figure 4.1. The darker lines directly connect fault lines between cores and deltas and lighter lines are virtual fault lines that indirectly connect cores and deltas. The relationship between cores and deltas can be described by the adjacent lists as shown in Figure 4.2 which cores are numbered first and deltas later.

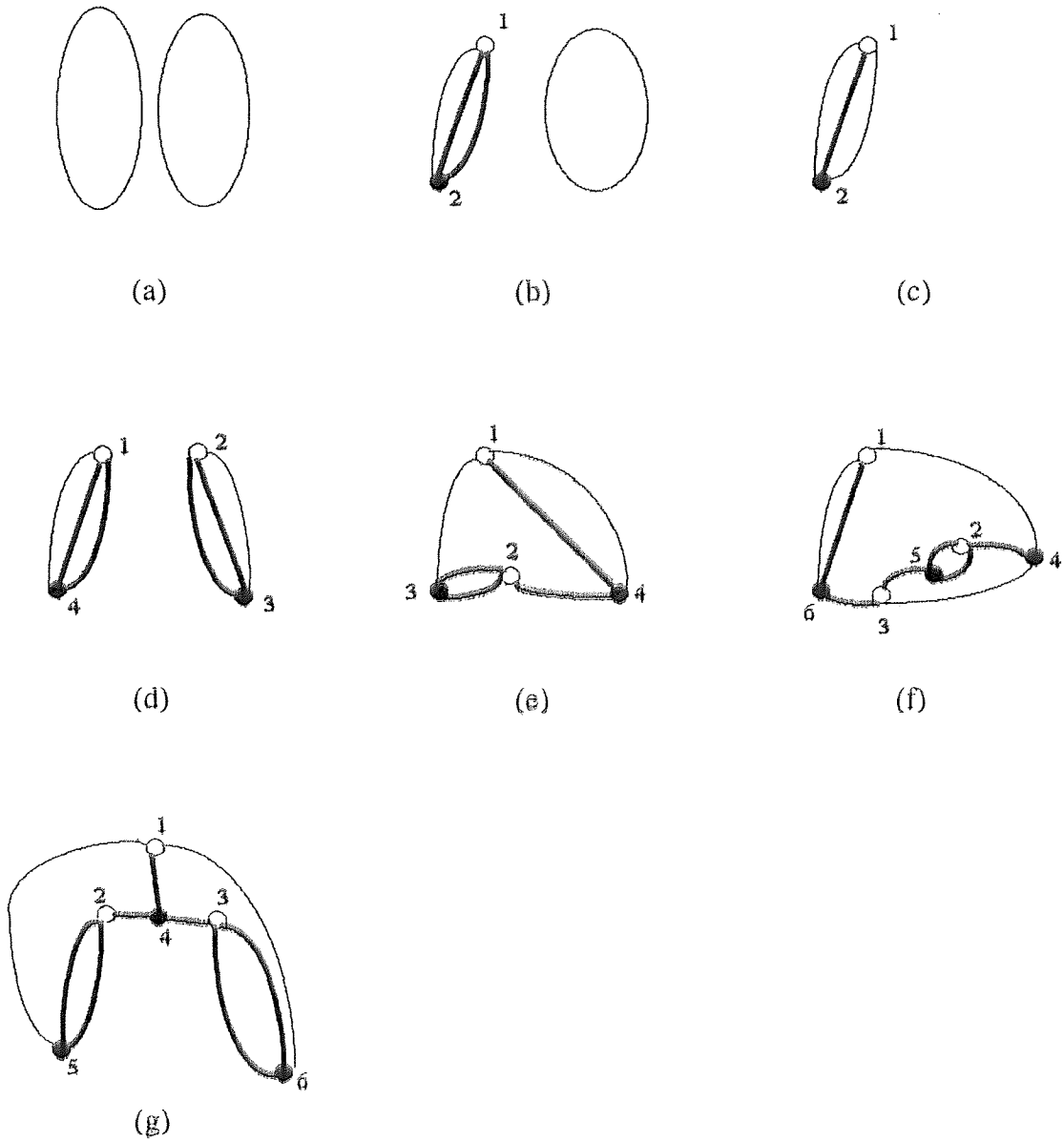

Figure 4.1 The *FLAG* of Figure 3.7. "o" and "•" indicates core and delta points, respectively. The darker and lighter lines are directly and indirectly connected fault lines between cores and deltas.

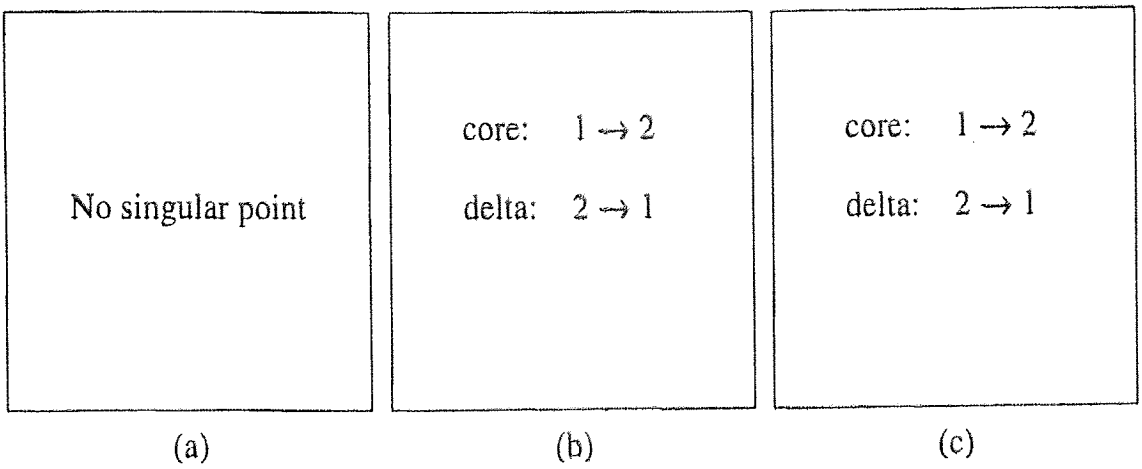

(a) (b) (c)

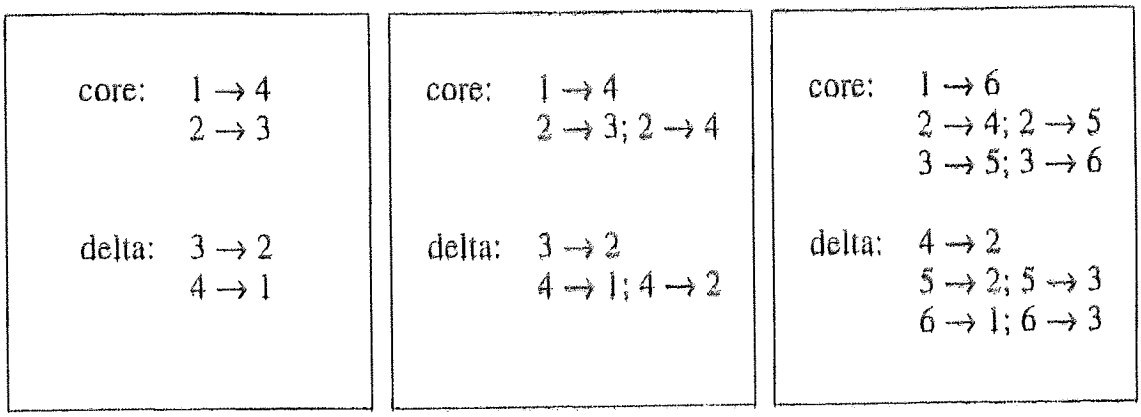

(d) (e) (f)

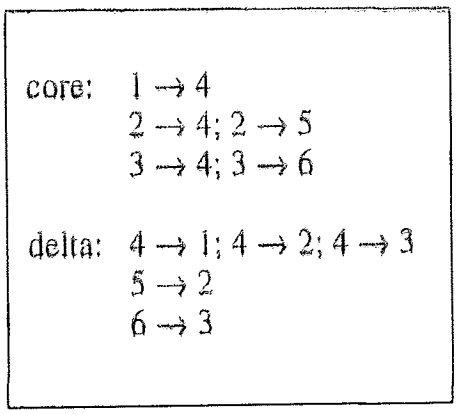

(g)

Figure 4.2 The adjacent list of Figure 4.1.

Theorem 4.1 A *FLAG* $G(C, D, E)$ is a bipartite graph.

Proof

In graph $G(C, D, E)$ there are only two kinds of nodes C and D. Therefore, we can model this graph G as 2-coloring graph. From Theorem 3.2, no fault line can be established between two singular points having an identical type. By McHugh [65], G is a bipartite graph.

Theorem 4.2 Singular points, exist in core-delta pairs.

Proof

Any given *FLAG* G is a bipartite graph. From the facts of Section 3.1.2, each singular point should be joined by exactly 3 fault lines. This indicates that graph G is a regular graph with degree 3 for vertices C and D [65]. We can conclude that graph G is regular and bipartite graph, so $|C| = |D|$. Graph G can be represented as an edge disjoint union of 3 complete matchings. Thus, a perfect matching can be applied to prove that cores and deltas must be matched. In other words, singular points show in core-delta pairs.

4.2 The Profile of Fingerprints

From chapters 3, we know that the global pattern of each fingerprint is decided by the geometric relationship of singular points which are formed by exactly 3 fault lines with $N = 3$. That means we can model the patterns of fingerprints by *FLAG*s.

According to Moayer and Fu [69], every fingerprint pattern has concave ridges on the top and nearly horizontal lines at the bottom. The concave ridges can be thought of being composed by 3 directions as shown in Figure 4.3. We has establish there is a fault line where there is a change of a direction. So, there must be fault lines between 0, 1, and 0, 2, cutting the concave ridges into 3 parts.

For the same reason, there will be two more cuts and two more fault lines on the left and right hand side when the concave ridge changes direction into near horizontal lines at

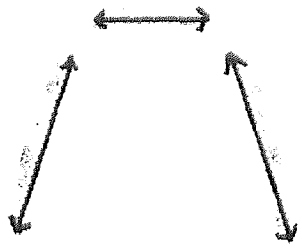

Figure 4.3 The concave ridge with 3 directions.

the bottom. As consequence there must exist 4 fault lines, *L*1, *L*2, *L*3 and *L*4, entering a pattern area on the fingerprint directional image. Figure 4.4(a) shows the layout of a fingerprint where we can consider its center as a region requiring further attention. Fault lines *L*1 and *L*2 or *L*3 and *L*4 may be merged like in Figure 3.7(a) or branch into more lines like other figures in Figure 3.7. These 4 fault lines are the free ends of all fault lines. Extending the definition by FBI [21], the "pattern area", the middle area of a fingerprint, in which the cores, deltas and ridges appear, determine the type of a fingerprint.

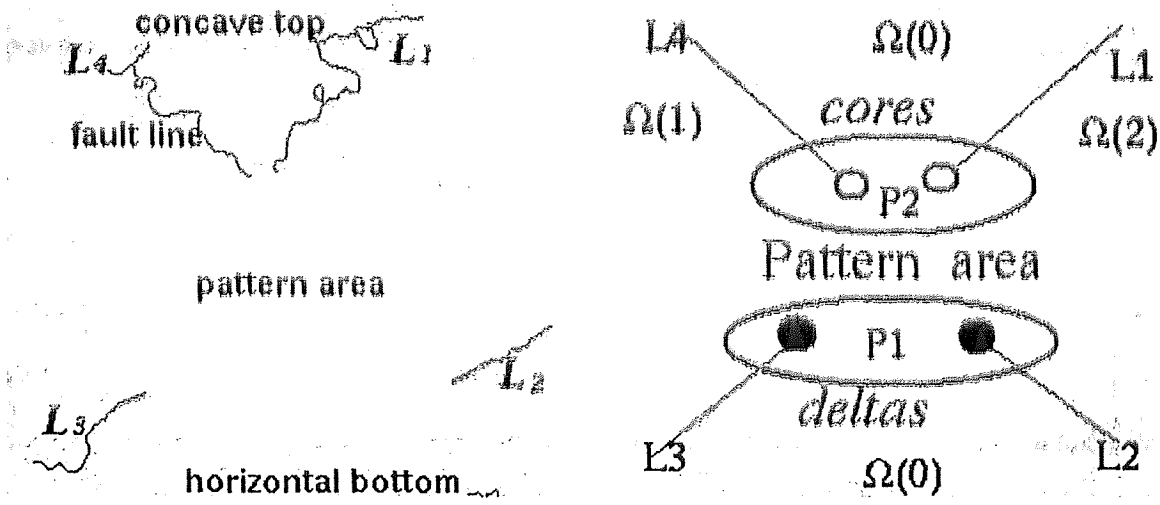

(a) (b)

Figure 4.4 (a) The logic profile of a fingerprint and (b) its pattern area. L1 and L2 will form cores, and L3 and L4 will form deltas. The numbers 0, 1 and 2 are indicated the direction regions Ω(0), Ω(1) and Ω(2).

Even though the singular point maybe missing (due to noise or any other reason), we can predict its type. From Section 3.2.1, we know that the directional patterns of a core point is any one of ''1 → 0 → 2'', ''0 → 2 → 1'' and ''2 → 1 → 0'', which the directional difference is +1 and -2, and a delta point is any one of ''0 → 1 → 2'', ''1 → 2 → 0'' and ''2 → 0 → 1'', which the directional difference is -1 and +2, in clock-wise direction manner around the singular point. Figure 4.4(b) is the enlarged part on the pattern area of Figure 4.4(a). There will be at least 4 directional regions, ''0'' at top and bottom, ''1'' at left, ''2'' at right, separated by the 4 fault lines.

The fault lines L1, L2, L3 and L4 are formed by shifted directions ''0 → 2'', ''2 → 0'', ''0 → 1'' and ''1 → 0'' in clock-wise direction, respectively. Matching with the patterns of singular points, we can find that L1 can only form a core point at the pattern area because the directional difference is -2. The same theory can be applied to L4 because the directional difference is +1. The fault line L2 can only form a delta point at the pattern area because the directional difference is +2, the same to L3 because the directional difference is -1. So, L1, L4 and L2, L3 are marked core and delta points at each end point at the pattern area of Figure 4.4(b).

4.3 Fingerprints Normalization

When fingerprints are imprinted, even if their orientation are manually adjusted, their orientations may shift within a certain range. Many research efforts have assumed that the orientation of the given fingerprints has been adjusted. In fact, the orientation of fingerprints may affect the efficiency and accuracy of classification and identification. To ensure the orientations of fingerprints are well within acceptable tolerance, rotation-normalization is necessary.

By Theorem 4.2, singular points have to exist in core-delta pair formations. The vector connecting the delta point to the core point will be referred as the *reference vector*. The reference vector is used to normalize a fingerprint by aligning it along the

horizontal direction using delta as the origin. For a fingerprint consisting of M core-delta pairs, there are M^2 reference vectors. Each normalized fingerprint using a selected reference vector is set as a valid candidate. Therefore, a *FLAG* containing 2 core-delta pairs, there are 4 reference vectors, and 4 valid templates will be established by the reference vectors.

Theoretically, a locality within a fingerprint is a unique pattern. It means the trajectories of all fault lines should be almost unique like the local ridge patterns. Recall that fault lines are places where ridge flows change directions and each singular point is the intersection point of fault lines. This implies that the fault lines configuration surrounding a core-delta pair can be represented as a locality of the ridge flows. In other words, a *FLAG* is a proper representation obtained from a normalized fingerprint.

The Exception: According to Henry's patterns [35], fingerprints having a plain arch type do not have singular points. In other words, there are no core-delta pairs to form the needed reference vectors as shown in Figure 4.5. To overcome this exception, a deformation function is needed to convert the plain arch type fingerprints into new patterns to generate the pseudo singular points. Thus, the reference vector can be constructed. Because there are many different kind of plain arch type fingerprints, the deformation function is very difficult to achieve. This technique will be subject of future work.

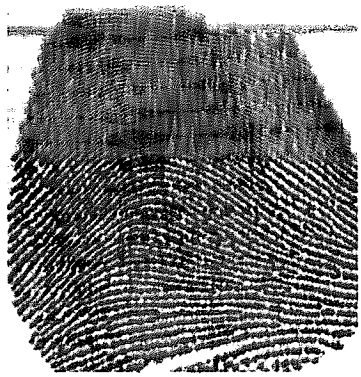

Figure 4.5 The plain arch type fingerprint (s0024611.wsq).

4.4 The Analysis of Normalization

Recall that the best result of a detected singular point is 2×2 pixels. This implies that the reference vector we selected may be not precise enough. This may cause a distortion in the singular point location after the rotation.

Given a *FLAG* $G(C, D, E)$, let τ be the positional displacement, L is the distance between D and C. Then the worst angular shifting is

$$\sigma = tan^{-1}(\frac{2\tau}{L-2\tau}) \qquad \sigma \simeq tan^{-1}(\frac{2\tau}{L}), \quad \text{if } L \gg 2\tau.$$

Figure 4.6 shows the relationship between σ and L under different τ. For example, L = 100, $\tau = 3$, the $\sigma = 3.65^{o}$.

By running 1700 images, the distance L is a normal distribution of (177, 59) under 500 dpi resolution (shown in Figure 4.7(a) with 4523 pairs.) We find that the core-delta pair (shown in Figure 4.7(b) with 3363 pairs) is more reliable than other kind of pairs because a core-delta pair has an average near 2 pairs per fingerprint. In contrast, the averages of delta-delta pairs (shown in Figure 4.7(c) with 529 pairs) and core-core pairs (shown in Figure 4.7(d) with 629 pairs) are less than half a pair per fingerprint.

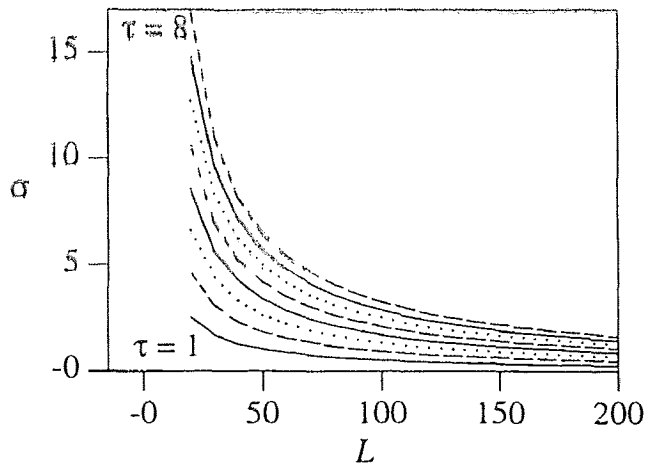

Figure 4.6 The relationship between σ and L under different τ, where σ is the tolerance to rotated angle θ, L is the distance of a core-delta pair, and τ is the tolerance of a singular point location.

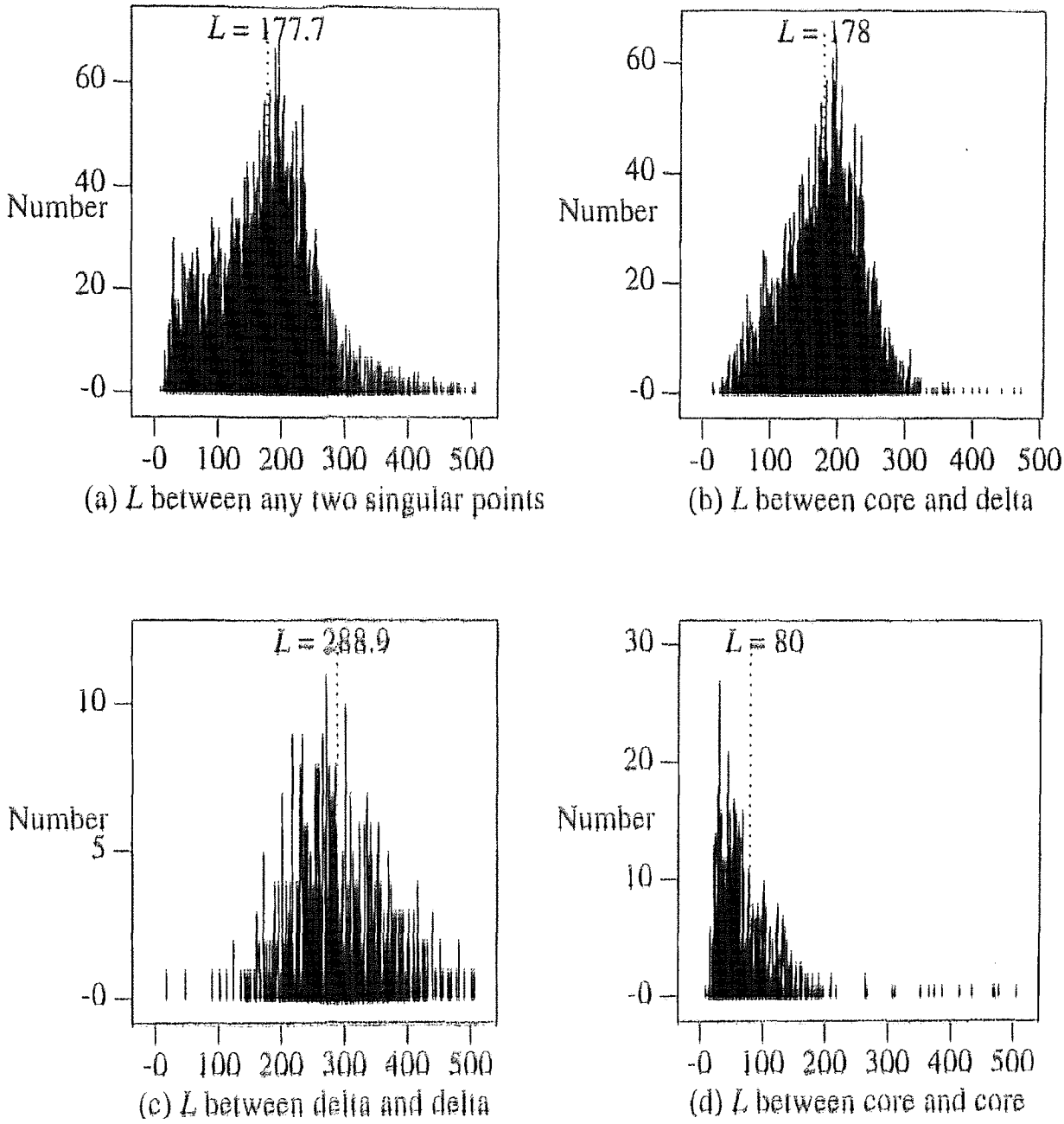

Figure 4.7 The histogram of L among the 4523 pairs of 1700 images. (a) All pairs with average L = 177.7. (b) Only between core and delta, with L = 178 in 3363 pairs. (c) Only between delta and delta, with L = 288.9 in 529 pairs. (d) Only between core and core, with L = 80 in 629 pairs.

Using the fingerprint image s0025432.wsq as our sample named as RS-0. Two templates of it are obtained by random rotations: one is named as RS-1 and the other is named as RS-2 as shown in Figure 4.8(b) and (c), respectively. Their reference vectors are shown in Figure 4.8(d), (e) and (f). Figure 4.8(g), (h) and (i) show the normalized *FLAG*.

On Table 4.1 shows the positions of core and delta points, reference vectors and distances L before the rotation. Each image is then re-oriented based on the computed reference angle θ. We apply the methods to re-process the rotated images and show the results in Table 4.2 with the new positions of core and delta points, rotated angle θ, new distances L and the normalized horizon vector. After normalization, the tolerances τ, σ and σ^* are show in Table 4.3. σ is the angle to horizontal and σ^* is the difference comparing with original rotated angle θ. It is obvious that the normalized images are almost the same image.

Table 4.1 The core and delta points before normalization.

	Core, Delta points	Reference Vector	L
RS-0(0^o)	(250, 176), (141, 341)	[109, -165]	197.5
RS-1(22^o)	(204, 200), (161, 391)	[43, -191]	195.8
RS-2(-32^o)	(292, 162), (112, 242)	[180, -80]	197.0

Table 4.2 The core and delta points with θ and new L after normalization.

	Core, Delta points	θ	New L	Horizon vector
org (0^o)	(302, 194), (106, 193)	-56.95^o	196.0	[196, 1]
RS-1(22^o)	(302, 192), (106, 194)	-77.54^o	196.0	[196, -2]
RS-2(-32^o)	(303, 199), (106, 201)	-23.96^o	197.0	[197, -2]

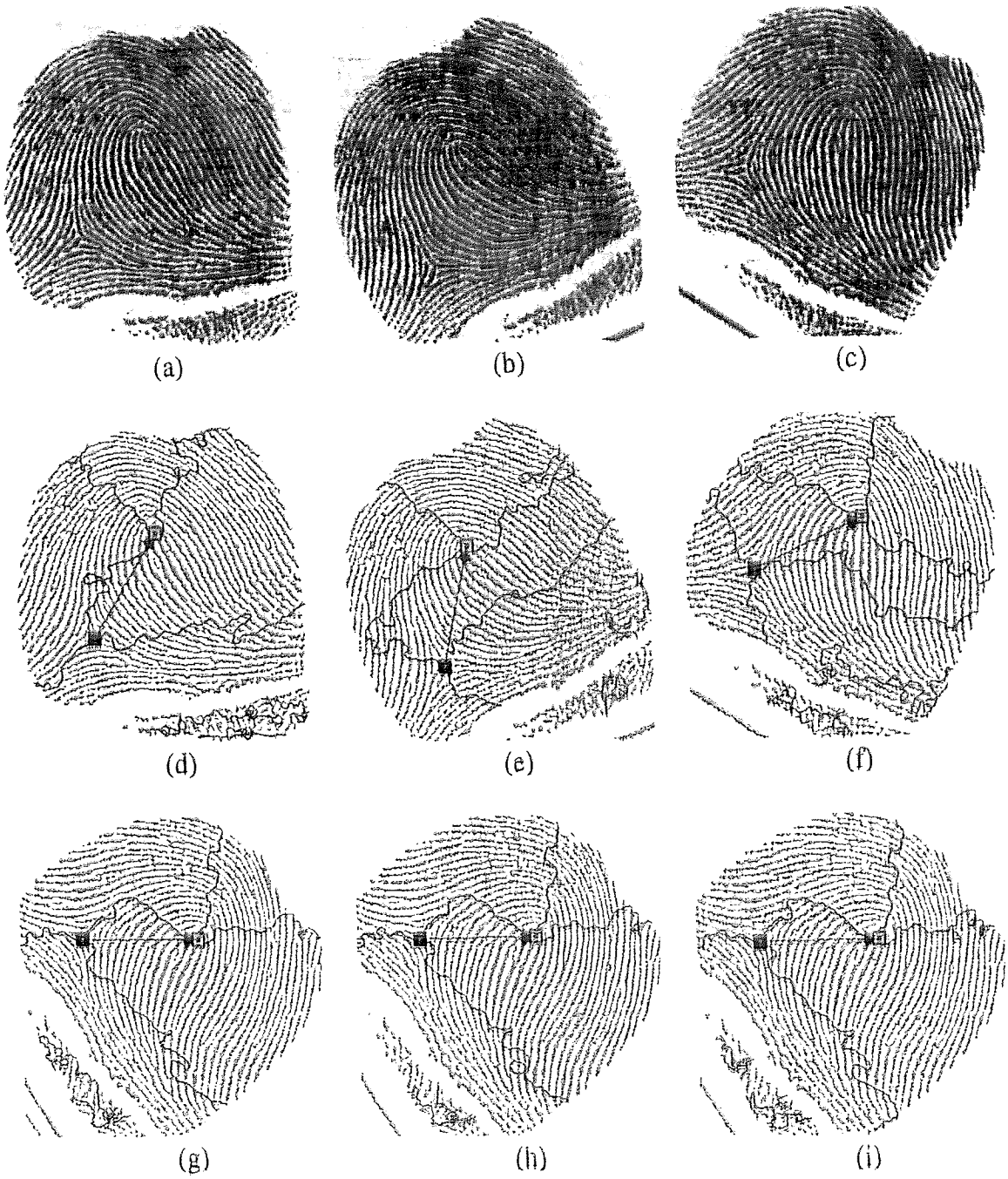

Figure 4.8 Random rotations of s0025432.wsq, (a) original, (b) 22^{o} and (c) -32^{o}. Their *FLAG*s with reference vector are shown in (d), (e) and (f). Their normalized *FLAG*s with horizon vectors are shown in (g), (h) and (i).

Table 4.3 The tolerances τ, σ and σ^*.

	τ	σ	σ^*
RS-0(0^o)	1	0.58^o	0^o
RS-1(22^o)	2	-1.16^o	1.41^o
RS-2(-32^o)	2	1.15^o	0.99^o

4.5 Conclusions

In this chapter, we prove that singular points must exist in core-delta pairs by a bipartite *FLAG*. We proposed a pattern model for fingerprints and the types of singular points can be predicted by our model. The automatic normalization is important to the correctness and precision of classification of fingerprints. A reference vector helps us to transform a fingerprint image to an invariant orientation. We analyzed the tolerance between several random rotations and the results show that the concept of the horizon vector works very well. With such well normalized *FLAG*, we can apply the characteristics of the *FLAG* model to classify fingerprints into more groups.

CHAPTER 5

THE MULTI-INDEX MODEL FOR FINGERPRINT CLASSIFICATION

The fingerprint classification is very important to the efficiency and accuracy of fingerprint identification. The current classification methods of fingerprints are based on Henry's categories which are pattern-oriented and the accuracy is based on visual justification. It is very hard to distinguish the difference between similar fingerprint patterns such as some tented arches and left (or right) loops. Therefore, precision and correctness is reduced and the time for identification is increased a lot. In this chapter, a new classification model is proposed based on the index attributes to renovate the current classification problems. The time of searching or matching process of fingerprints can be reduced significantly for huge databases using our models, fingerprints can be divided into hundreds of thousands of smaller groups which are based on the attributes of horizon vectors in the normalized *FLAG*s.

5.1 The Classification Model

It has been difficult to increase the number of classification groups because there was no way to precisely detect the position of the singular points, and therefore, it was not possible to establish the relationships between them. We can classify fingerprints into hundreds of thousands groups by the index attributes which are the geometric relationship in normalized horizon vectors.

5.1.1 The Current Problems

As previously mentioned, when the number of fingerprint records is large, the current methods are not fast enough to process the required fingerprints. The reason is because currently there are only a few groups (less than ten) to classify fingerprints so that each

group contains a large amount to manage. The three major types of Henry's classification are arch, loop and whorl, and these 3 types can be divided into several subcategories. In addition, the classification of Henry's system is pattern oriented and the correctness is based on visual justification. It is very difficult to distinguish between some fingerprints. Figure 5.1 shows the ambiguous type of fingerprints that they are difficult to be classified as tented arch or as left loop types of fingerprints [35], especially when they they are not well oriented. They are so similar that it is necessary to search in the both groups of tented arch and left loops when the identification process is applied.

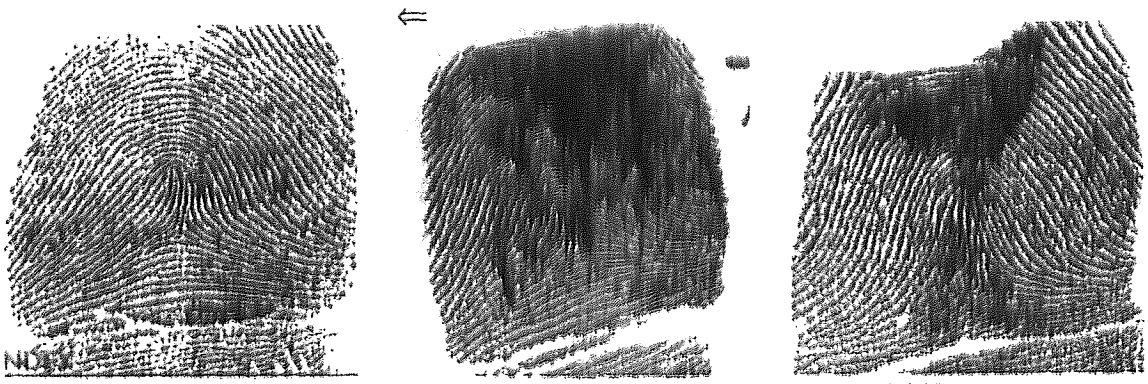

(a) s0025552.wsq (b) s0026572.wsq (c) s0026622.wsq

Figure 5.1 The ambiguous types of fingerprints.

Kurre [24] stated that the total number of fingerprints increased 12.5% over the year 1996. This means that the total number of total records will more than double in less than a decade. Currently, the FBI has more than 219 million fingerprints which each group may contain an average of 21 millions of records in Henry's system with assuming there is a uniform distribution. Just provide an idea how many fingerprints need to be processed if the type of a fingerprint is a ambiguous like Figure 5.1. The current AFIS needs to be manually judge and check it in these two groups with combing into 44 million fingerprints.

5.1.2 The Attributes of a *FLAG*

For each normalized horizon vector, we can extract the attributes from the *FLAG*. We can build the model consisting of the horizon vector, the fault lines and the relationship between them. Figure 5.2 illustrates this concept. This model contains three important attributes such as the trajectories of the fault lines connecting the core-delta pair the length of the horizon vector, and the number of ridges crossed by the horizon vector; what are the attributes and how to discover them is important to the classification model. Theoretically, the fault line trajectories should represent the direction change of ridge flows and they should change smoothly. A stable and reliable attribute is important to help describe the trajectories.

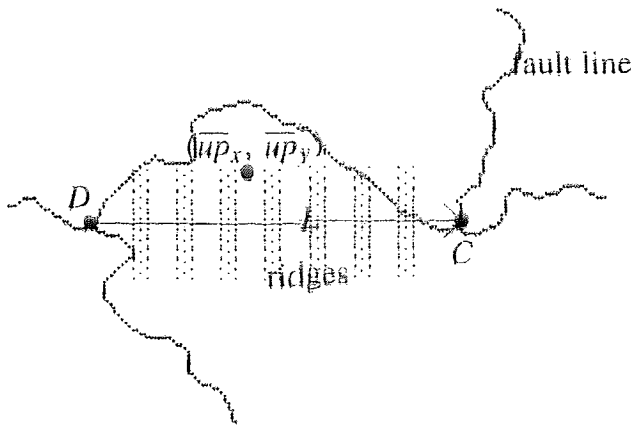

Figure 5.2 The horizon vector of a *FLAG*.

We can quantize the attributes of a *FLAG* into integer numbers in order to reduce the noise. We can think each attributes as the combination of correct and error quantities as

$$A_i = c_i + e_i.$$

A quick way to reduce the error in significant amount is to divided the attributes by constant λ as

$$A_i = \frac{c_i}{\lambda_i} + \frac{e_i}{\lambda_i}.$$

This constant has to be large enough such that $\frac{e_i}{\lambda}$ becomes insignificantly and the same time small enough such that $\frac{c_i}{\lambda_i}$ remains meaningful. We can think the constant λ_i as the UNIT for its respect attribute. Let $n_i = \lceil \frac{c_i}{\lambda_i} \rceil$, where n_i represents the normalized range of the attribute A_i. Then, the attributes can be described as a tuple

$$(A_1, A_2, ..., A_k, ...,A_m), \text{ where } A_i \in [0, n_i-1],\ 1 \le i \le m.$$

5.1.3 The Candidate Attributes

By our experiments, the attributes can be the following

- L is the length of the horizon vector.
- R is the number of ridges crossing by the horizon vector.
- $\overline{up}_y$ is the pixels' average of y coordinates within the area between pair vector and the fault line which is *above* the horizon vector.
- $\overline{up}_x$ is the pixels' average of x coordinates within the area between pair vector and the fault line which is *above* the horizon vector and their $y \ge \overline{up}_y$.
- $\overline{dn}_y$ is the pixels' average of y coordinates within the area between pair vector and the fault line which is *below* the horizon vector.
- $\overline{dn}_x$ is the pixels' average of x coordinates within the area between pair vector and the fault line which is *below* the horizon vector and their $y \ge \overline{dn}_y$.

By running 1700 images, we have the the characteristics, average, standard deviation, minimum and maximum values, and the 95% distributed ranges. of each attribute resolution listed in Table 5.1.

Table 5.1 The characteristics of each attribute under 500 dpi resolution.

Attributes	Mean	S.D	(min, max)	95% Population
L	177.5	59.5	(16, 468)	(56, 294.5)
R	13.9	5.4	(1, 36)	(3.1, 24.7)
$\overline{up}_y$	47.2	36.4	(0, 170)	(0, 119)
$\overline{up}_x$	86.5	38.8	(0, 230)	(8.9, 164)
dn_y	32.4	28.4	(0, 154)	(0, 89.1)
dn_x	84.6	33.7	(0, 190)	(17, 152)

5.2 The Multi-Index Classification

With the normalization, the attributes are represented by discrete numbers. An array structure can be applied to store the attribute and the corresponding address.

5.2.1 The Index Tree

A tree structure can be used to represent the relationship between the attributes. The root and each internal node are arrays using the normalized attribute values as index to store the corresponding address of the node in the next level. Each leaf contains the finger-prints in the same class. The final matching process takes place in a certain leaf.

The variables of a attribute ${}_jA_{h,\,i}$ defined as the follow.

- h is the index level of the current attribute.
- i is the order number in index level h of the current attribute.
- j is the order number in index level j of the parent attribute of the current attribute.
- $f({}_jA_{h,\,i})$ is the address of the child attribute.

If there are m attributes as $(A_1, A_2, ..., A_k, ...,A_m)$, the multi-index classification tree of these attributes is shown in Figure 5.3. For k-th level which represents a attribute

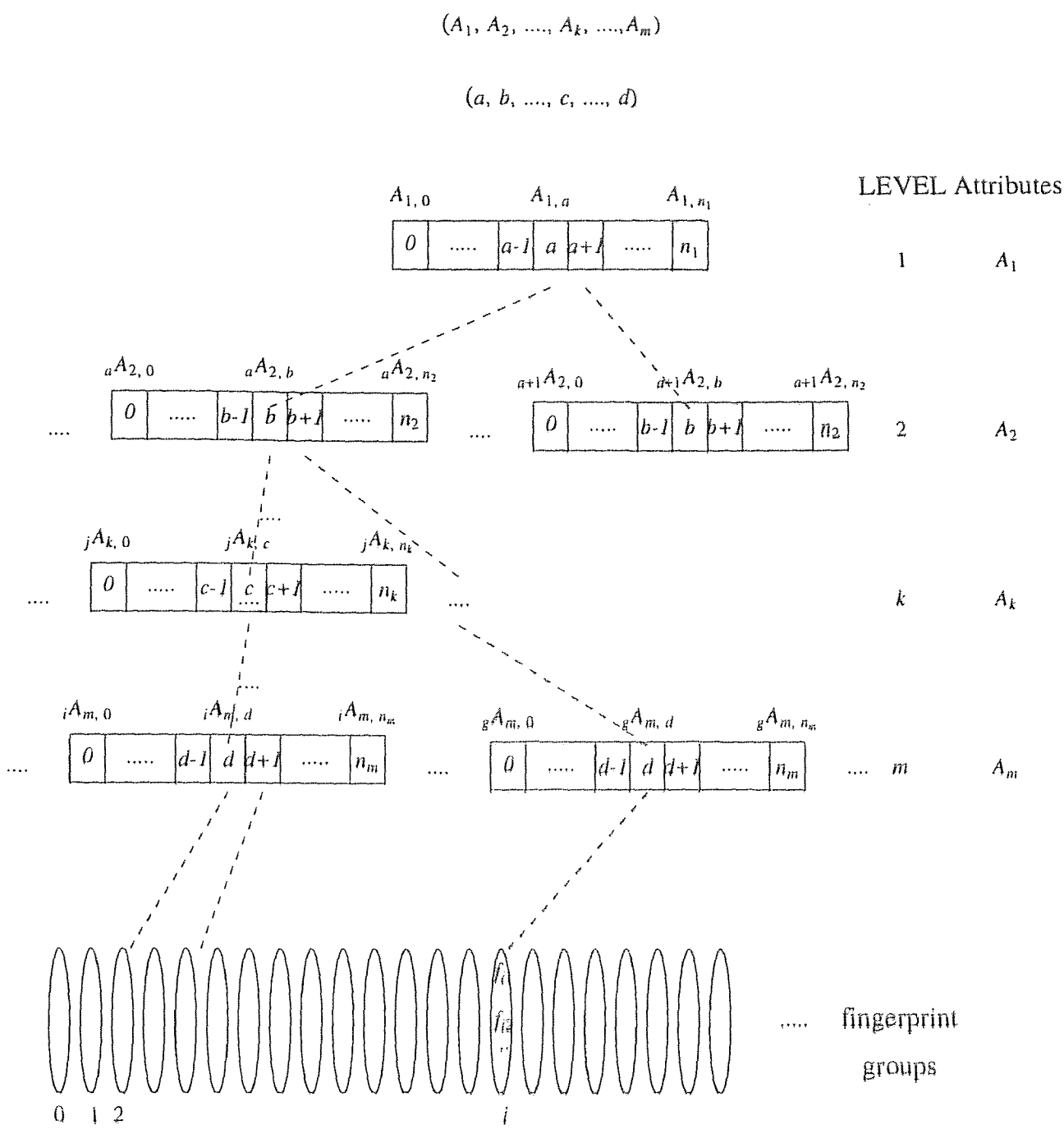

Figure 5.3 The Multi-Index Classification Tree.

A_k, it has n_{k-1} arrays which each array has same index number n_k of entries and structures. Every array contains the normalized range of the attribute A_k in level k as from 0 to n_k. The first level has only one array. The number of classified groups will be

$$\prod_{i=1}^{m} n_i.$$

That means, the fingerprint groups will be numbered from 1 to $n_1 \times n_2 \times \ldots \times n_k \times \cdots \times n_m$. Although the best candidate group is directly hit, it is necessary to consider the noisy effect. The tolerance μ_k will be applied to the numerical description in level k when it is re-mapping in the multi-index classification tree. So, the number of groups need to check will be

$$\prod_{i=1}^{m} (2\mu_i+1).$$

If we only consider to check the right and left neighbor of an attribute A_k, the tolerance μ_i will be 1. Given attributes (a, b, ..., c, ..., d) and the tolerance μ of attributes is 1, the groups of tuple descriptions for checking will be ($a\pm1$, $b\pm1$, ..., $c\pm1$, ..., $d\pm1$). For example, given a tuple description (8, 4, 20, 32, 0, 0), its multi-index classification tree is shown in Figure 5.4 and there will be 324 possible checking groups against the all groups. The searching will be stopped when there is a match. If the input fingerprint cannot be found in the possible groups, we claim that it does not exist in the database.

5.2.2 Example of Classification

From Section 5.1.3, a fingerprint can be described by the index attributes as

$$(L, R, \overline{up}_y, \overline{up}_x, \overline{dn}_y, \overline{dn}_x).$$

The estimated number of combinations for each horizon vector will be

$$n_L \times n_R \times n_{\overline{up}_y} \times n_{\overline{up}_x} \times n_{\overline{dn}_y} \times n_{\overline{dn}_x}.$$

In our experiments we use $\lambda_L = 10$, $\lambda_R = 2$, $\lambda_{\overline{up}_y} = 5$, $\lambda_{\overline{up}_x} = 5$, $\lambda_{\overline{dn}_y} = 5$, and $\lambda_{\overline{dn}_x} = 5$. Using the maximum range in Table 5.1, we can have the maximum estimated number of total groups as: $48 \times 19 \times 47 \times 35 \times 39 \times 32 = 1{,}872{,}299{,}520$. In other words, the possibility for the same tuple description is less than 1.8 billionth. Using the average range in Table 5.1, we can have the average estimated number of total groups as: $19 \times 8 \times 18 \times 10 \times 18 \times 7 = 3{,}447{,}360$. In other words, the possibility for the same tuple description is less than 6.5 millionth.

5.3 Experiments

Given several similar fingerprints which are classified as right loops in Henry's system in Figure 5.5, their tuple descriptions are listed on the bottom of each image. We can find that the fingerprints are very similar if their tuple descriptions are similar. Different orientation of same fingerprints will have the same tuple description such as Figure 5.5 (c). Given other 3 images with different number of core-delta pairs which are from Figure 1.2 (e), (g) and (h), their tuple descriptions are shown under the Figure 5.6 (a), (b) and (c).

Our database consists of the 1700 images of fingerprints which are part of the NIST PCASYS package, in addition to 50 fingerprints collected from our friends. We re-scanned the donated 50 images again as our wanted fingerprints, we run our classification program, we obtain the 48 fingerprints classified in the same group as their original counterpart. Only two fingerprints did not fell into the same group, however, their classification was within $\mu = 1$. The result gives a good proof of the direction of our classification model.

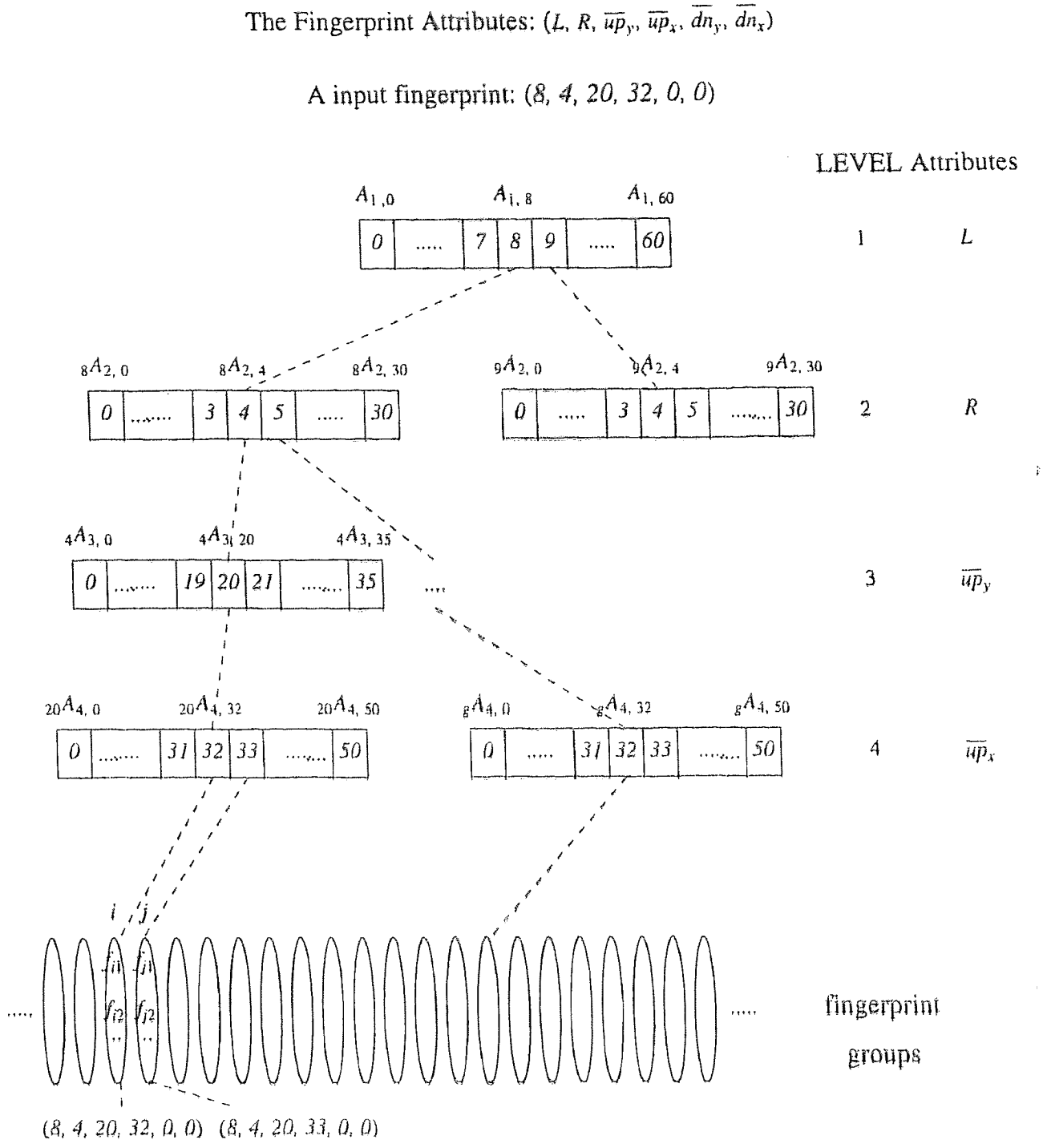

Figure 5.4 The Multi-Index Classification Tree of a tuple description (8, 4, 20, 32, 0, 0).

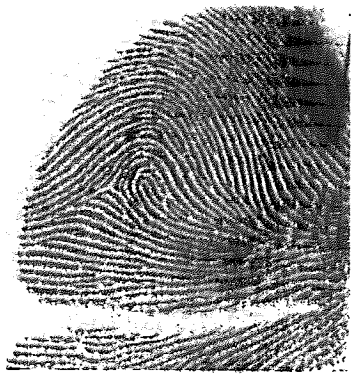

(a) s0025112.wsq
(5, 2, 3, 4, 2, 5)

(b) s0025504.wsq
(6, 3, 3, 4, 0, 0)

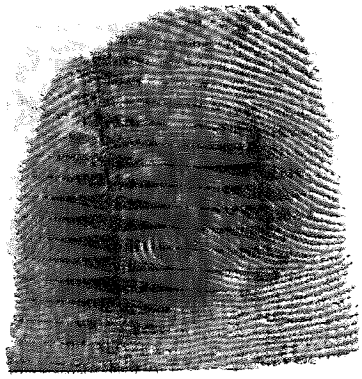

(c) s0026411.wsq
(10, 4, 3, 9, 2, 9)

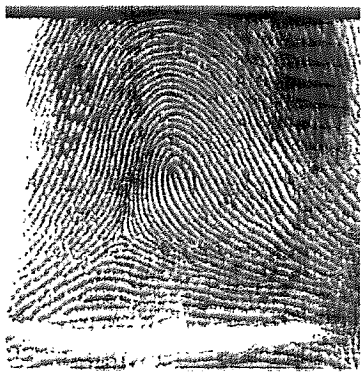

(d) s0025453.wsq
(12, 3, 0, 12, 0, 0)

(e) s0024384.wsq
(12, 6, 4, 13, 0, 0)

(f) s0025943.wsq
(14, 5, 3, 16, 0, 0)

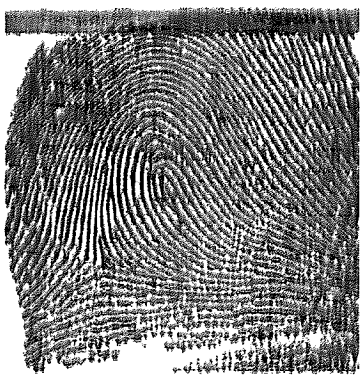

(g) s0026873.wsq
(16, 6, 6, 16, 0, 0)

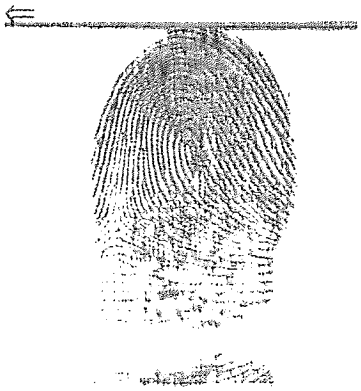

(h) s0025123.wsq
(16, 6, 7, 18, 0, 0)

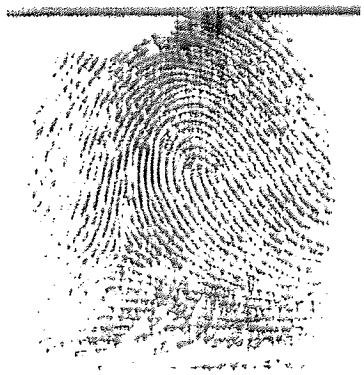

(i) s0025823.wsq
(16, 6, 12, 17, 0, 0)

(j) s0025451.wsq
(16, 7, 12, 4, 3, 14)

(k) s0025432.wsq
(20, 7, 6, 18, 0, 0)

(l) s0024355.wsq
(20, 9, 13, 21, 0, 0)

Figure 5.5 The tuple descriptions of similar right loop types of fingerprints.

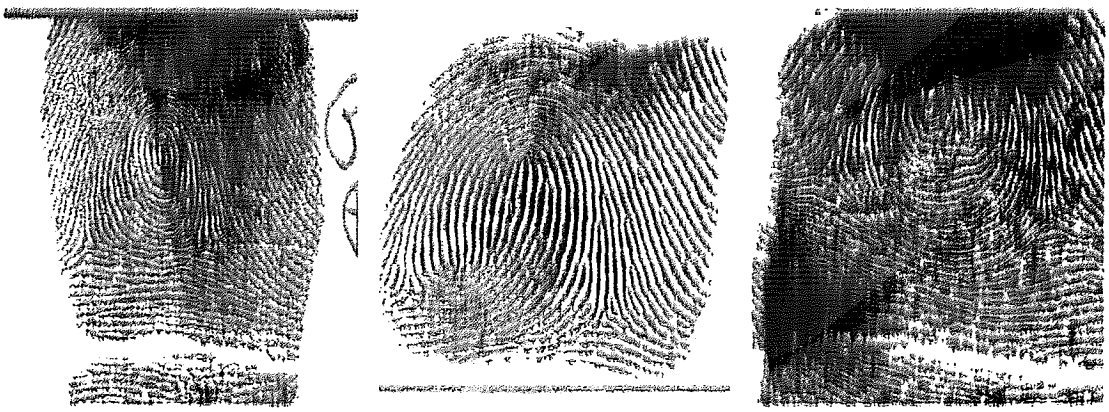

(a) s0025024.wsq
(9, 4, 12, 20, 6, 11)
(17, 8, 5, 17, 0, 0)
(16, 7, 0, 0, 2, 14)

(b) s0024902.wsq
(6, 2, 3, 7, 2, 5)
(24, 5, 0, 0, 4, 22)
(23, 9, 8, 23, 12, 21)

(c) s0024967.wsq
(6, 2, 0, 0, 0, 6)
(5, 2, 0, 0, 0, 0)
(2, 1, 0, 0, 0, 2)
(15, 7, 0, 0, 5, 11)
(15, 7, 3, 16, 0, 0)

Figure 5.6 The tuple descriptions contain different core-delta number.

The partial matching will be done if there exists a core-delta in fingerprints. For future work, we will study on the attributes of the other two kind of pairs, core-core and delta-delta, so that make the partial matching more solid.

5.4 Conclusions

In this chapter, we represent a fingerprint as a sequence of numerical attributes. We can classify fingerprints into millions of groups by the attributes. This is a totally new concept to fingerprints. With such an outstanding classification, the time for searching and comparing will be reduced to significantly because the possible fingerprints are narrowed down into a very small number. Furthermore, the partial matching for incomplete fingerprints is within reach.

CHAPTER 6

CONCLUSION

6.1 Summary of Results

The results of this dissertation about fingerprint analysis, feature extraction, pattern modeling and re-orientation, and classification are presented below:

- *Fuzzy techniques for flow oriented image direction computing.* This is a state-of-art technique to process flow oriented images such as fingerprints, elevation of mountain and magnetic field. A fuzzy template is designed to speedup and get better directional images. We proved that directional number $N = 3$ will yield the better quality results for fingerprints.
- *Pyramidal model for detecting singular points.* Singular points are the global features of fingerprints. We designed a fast algorithm to detect almost pinpoint locations of singular points and classify them as cores or deltas by pattern templates. We prove that fault lines only intersect at singular points, and do not connect singular points of the same type.
- *The FLAG and the fingerprints normalization.* We proposed a Fault Line Graph (*FLAG*) to represent a fingerprint. The analysis of the pattern area of *FLAG*s will help us predict the location of singular points. We prove that the *FLAG* is a bipartite graph and singular points must exist in core-delta pairs. We transform fingerprints into invariant orientation by the pair vector so that the correctness of classification will be improved.
- *The New classification model.* Based on our new classification techniques, the fingerprints can be classification into hundreds of thousands groups by the mathematic attributes of core-delta pairs. With such an outstanding classification, the

time of searching in a huge database can be done in a very short time, and the partial matching can be made more possible.

6.2 Future Research Direction

As always, successful research and development opens up new research areas and opportunities. While invariant approaches have achieved a certain level of maturity, advances are expected along several lines of investigation.

First, the type of the plain arch fingerprint needs more study to do the normalization and to discover the attributes like the *FLAG*. So, the new classification model will completely cover all different types of fingerprints.

Next, although the partial matching is made more possible by our pattern modeling and classification techniques, it needs more research to achieve real time performance not only theoretically but practically.

Finally, although our algorithms has been successfully tested under a small database because of limited resources, it would better to apply them to a huge database for further test and improvement.

APPENDIX A

THE EXTRACTION OF FINGERPRINTS

Since fingerprints are scanned into images from the stored cards which may contain some noise, The bigger images and consequent noise will reduce the processing performance and require more memory and space. So, it is necessary to extract the essential contents, containing only the fingerprints.

The Diffusion

First, we need to assume that the extracted image N with size $N_n \times N_n$ is bigger than any other object on a fingerprint card image M which size is $M_x \times M_y$. We define some functions and terms as followings.

- U_{ij}: Represents the gray level at position (j, i) of the image U.
- $G(U, x1, y1, x2, y2)$: Returns the average gray level of the rectangle area from $(x1, y1)$ to $(x2, y2)$ on the image U, and both positions are included.
- $MIN(U, x1, y1, x2, y2)$: Returns the minimum gray level of the rectangle area from $(x1, y1)$ to $(x2, y2)$ on the image U, and both positions are included.
- *thr*: The critical value to be an object is assigned by the maximum one between $M_x/10$ and $M_y/10$.
- *position*(*hist*, $x1$, $x2$, *thr*): returns the first position of the longest continuous length on *hist* list from position $x1$ to $x2$ and each number is greater than *thr*.
- We assume that gray level 0 as object, 255 as background.

Then we calculate the histograms *histx* and *histy* which are along the x- and y-axis direction on the diffused image M by the following algorithm:

average = $G(M, 0, 0, M_x-1, M_y-1)$
for(i=0; $i< M_y$; i++)
for(j=0; $j< M_x$; j++)
  if $G(M, j-1, i-1, j+1, i+1) <$ *average* then
    { *histx[j]*++; *histy[i]*++; }

The extracted positions will depend on the *histx* and *histy* with *thr*.

- *min_x* = *position*(*histx*, 0, M_x-1, *thr*);
- *max_x* = *position*(*histx*, M_x-1, 0, *thr*);
- *min_y* = *position*(*histy*, 0, M_x-1, *thr*);
- *max_y* = *position*(*histy*, M_x-1, 0, *thr*);

Then we have the temporary starting (*min_x*, *min_y*) and ending (*max_x*, *max_y*) position for the new image N from the image M.

The Adjustment

Since we want to have a fixed size output $N_n \times N_n$, it is very possible that (*max_x* - *min_x*) or (*max_y* - *min_y*) is bigger or smaller than N_n. We need to locate better positions to focus only on the fingerprint. The adjusting process is described as follows:

if $min\_x < 0$ then $min\_x = 0$;
if $min\_y < 0$ then $min\_y = 0$;
if $max\_x > M_x$ then $max\_x = M_x$;
if $max\_y > M_y$ then $max\_y = M_y$;
if $max\_x - min\_x < N_n$ then $max\_x = min\_x + N_n$;
if $max\_y - min\_y < N_n$ then $max\_y = min\_y + N_n$;
if $max\_x > M_x$ then $\{max\_x = M_x; min\_x = max\_x - N_n\text{-}1; \}$
if $max\_y > M_y$ then $\{max\_y = M_y; min\_y = max\_y - N_n\text{-}1; \}$
$N_x = max\_x - min\_x$; $N_y = max\_y - min\_y$;

The new adjusted image N will cover from (*min_x*, *min_y*) to (*max_x*, *max_y*) of image M.

APPENDIX B

THE SEGMENTATION OF FINGERPRINTS

Most fingerprint processes require only two levels: object and background. Some of images or portions of an image may be too light, and some of them may be too dark. This is a common problem with image processing, but especially in fingerprints because of their latent characteristics. Improper threshold will generate false or remove important minutiae such as bifurcations, islands and bridges. Therefore, how to get better thresholded image is an important subject to fingerprints. The new thresholded images B will be segmented from N by the following algorithm.

```
average1 = G(N, 0, 0, Nx−1, Ny−1)
for(i=0; i< Ny; i++)
  for(j=0; j< Nx; j++)
    if G(N, j−2, i−2, j+2, i+2) > average then
    {
      if G(N, j−2, i−2, j+2, i+2)+1 ≥ G(N, j−1, i−1, j+1, i+1) AND
      MIN(N, j−2, i−2, j+2, i+2)+1 ≤ average1 then
            Bij = 0;
      else
      {
        if MIN(N, j−1, i−1, j+1, i+1)+1 ≤ (average1 + average)/2.0 + 1 AND
        MIN(N, j−1, i−1, j+1, i+1) + (average - average1)/2.0+1 ≥ Nij then
            Bij = 0;
        else
            Bij = 255;
      }
    }
    else
    {
      if MIN(N, j−2, i−2, j+2, i+2)+1 ≤ average +1 AND
      G(N, j−2, i−2, j+2, i+2)+1 ≥ G(N, j−1, i−1, j+1, i+1) +1 then
            Bij = 0;
      else
            Bij = 255;
      }
```

The image B will be the final thresholded output with fixed size $N_n \times N_n$. Using s0024673.wsq from the test database demonstrates the extracting process, Figure A(a) is

the original scaled image, (b) and (c) are the histograms *histx* and *histy* of the diffused image (a). The dotted lines of (b) and (c) show the *min_x*, *max_x* and *min_y*, *max_y*, respectively. (d) is the adjusted result. (e) is the segmented result.

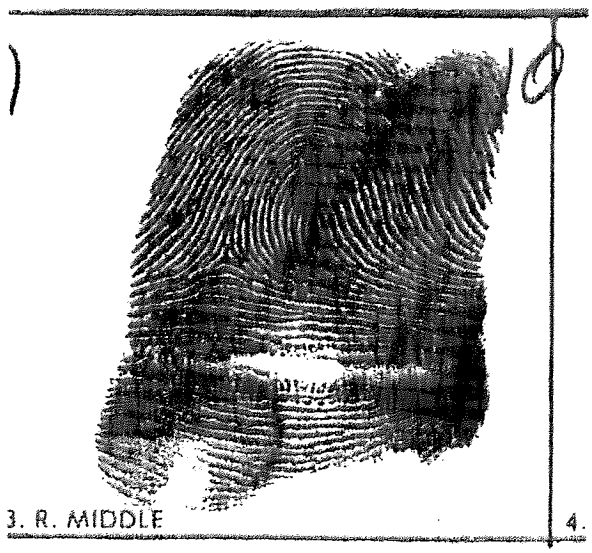

(a)

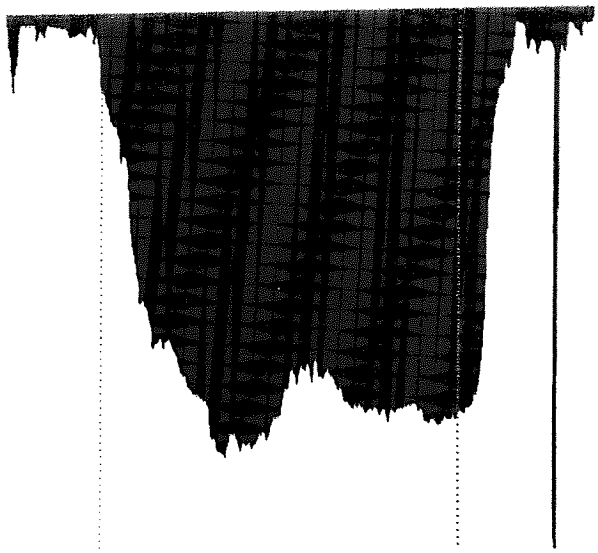

(b)

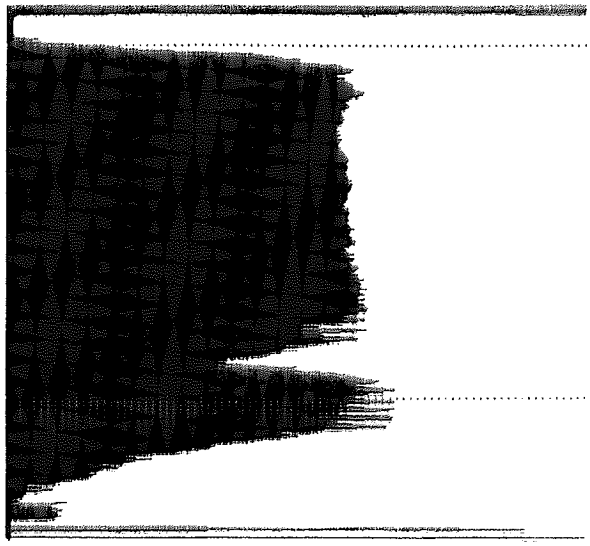

(c)

(d)

(e)

Figure A Using s0024673.wsq from NIST as our experiment. (a) The original image. (b) The *histx*. (c) The *histy*. (d) The result after adjustment. (e) The final thresholded image.

REFERENCES

[1] American National Standards Institute (ANSI), *Fingerprint Identification - Data Format for Information Interchange*. New York, NY: ANSI, 1986.

[2] Carlo Arcelli and Gabriella Sanniti Di Baja, "A Width-Independent Fast Thinning Algorithm," *IEEE PAMI*, vol. 7, no. 4, pp. 463 - 474, July 1985.

[3] O. Baruch, "Line Thinning by Line Following," *Pattern Recognition Lett.*, vol. 8, pp. 271 - 276, 1988.

[4] J. L. Blue, G. T. Candela, P. J. Grother, R. Chellappa and C. L. Wilson, "Evaluation of Pattern Classifiers for Fingerprint and OCR Applications," *Pattern Recognition*, 27, pp. 485 - 501, 1994

[5] Jonathan N. Bradley and Christopher M. Brislawn, "The FBI Wavelet/Scalar Quantization Compression Standard for Digital Fingerprint Images," in *Proc. Nat'l Media Lab Conf. Solid-State Memory*, Pasadena, CA, 1996.

[6] Jonathan N. Bradley and Christopher M. Brislawn, "The Wavelet/Scalar Quantization Compression Standard for Digital Fingerprint Images," in *Proc. IEEE ISCAS-94*, London, 1994.

[7] A. D. Brink, "Grey-level Thresholding of Images using a Correlation Criterion," *Pattern Recognition Lett*, vol. 9, pp. 335 - 341, 1989.

[8] R.M. Brown, T.H. Fay and C.L. Walker, "Handprinted Symbol Recognition System," *Pattern Recognition*, vol. 21, no. 2, pp. 91 - 118, 1988.

[9] G. T. Candela and R. Chellappa, "Comparative Performance of Classification Methods for Fingerprints," National Institute of Standards and Technology (NIST) Technical Report 5163, Image Recognition Group, Advanced Systems Division, NIST, US Dept. of Commerce, Apr. 1993.

[10] G. T. Candela, P. J. Grother, C. I. Watson, R. A. Wilkinson and C. L. Wilson, "PCASYS - A Pattern-Level Classification Automation System for Fingerprints," National Institute of Standards and Technology (NIST) Technical report 5647, Image Recognition Group, Advanced Systems Division, NIST, US Dept. of Commerce, Aug. 1995.

[11] T. Ch and Malleswara Rao, "Feature Extraction for Fingerprint Classification," *Pattern Recognition*, vol. 8, pp. 181 - 192, 1976.

[12] Shih-Hsu Chang, Fang-Hsuan Cheng, Wen-Hsing Hsu and Guo-Zua Wu, "Fast algorithm for Point Pattern Matching: Invariant to Translations, Rotations and Scale Changes," *Pattern Recognition*, vol. 30, no. 2, pp. 311 - 320, 1997.

[13] C. E. Chapel, *Fingerprinting - A Manual of Identification*. New York, NY: Coward McCann, 1971.

[14] Michael M. S. Chong, Robert K. L. Gay, H. N. Tan, and J. Liu, "Automatic Representation of Fingerprints for Data Compression by B-Spline Functions," *Pattern Recognition*, vol. 25, no. 10, pp. 1199 - 1210, 1992.

[15] Louis Coetzee and Elizabeth C. Botha, "Fingerprint Recognition in Low Quality Images," *Pattern Recognition*, vol. 26, no. 10, pp. 1441 - 1460, 1993.

[16] J. F. Cowger, *Friction Ridge Skin: Comparison and Identification of Fingerprints*. New York, NY: Elsevier, 1983.

[17] Peter J. Denning, Jack B. Dennis and Joseph E. Qualitz, *Machines, Languages and Computation*. Englewood Cliffs, NJ: Prentice-Hall, 1978.

[18] Didier Dubois and Henri Prade, "Fuzzy Sets - A Convenient Fiction for Modeling Vagueness and Possibility," *IEEE Trans. Fuzzy Systems*, vol. 2, no. 1, pp. 16 - 21, Feb. 1994,

[19] M. Eleccion, "Automatic Fingerprint Identification," *IEEE Spectrum*, 10, pp. 36 - 45, 1973.

[20] Federal Bureau of Investigation (FBI), "The State of Development of The FBI's automatic Fingerprint Identification System," FBI Law Enforcement Bill, June, 1973.

[21] Federal Bureau of Investigation (FBI), "The Science of Fingerprints: Classification and Uses," FBI Report, U.S. Goverment Printing Office, Washington, D.C., 1984.

[22] Federal Bureau of Investigation (FBI), "Fingerprint Identification," FBI Report, U.S. Goverment Printing Office, Washington, D.C., 1991.

[23] Office of Technology Assessment (OTA), "The FBI Fingerprint Identification Automation Program: Issues and Options," OTA Report, Congress of the United States, 1991.

[24] Dennis G. Kurre, "Fingerprint Identification and Related Information Services,", Statement of Dennis G. Kurre, Deputy Assistant Director, Criminal Justice Information Services Division, FBI, to U.S. House of Representatives, Apr. 30, 1997.

[25] Kenneth H. Fielding, Joseph L. Horner and Charles K. Makekau, "Optical Fingerprint Identification by Binary Joint Transform Correlation," *Optical Engineering*, vol. 30, no. 12, pp. 1958 - 1961, Dec. 1991.

[26] A. P. Fitz and R. J. Green, "Fingerprint Classification Using a Hexagonal Fast Fourier Transform," *Pattern Recognition*, vol. 29, no. 10, pp. 1587 - 1597, 1996.

[27] King-Sun Fu and Bharat K. Bhargava, "Tree Systems for Syntactic Pattern Recognition," *IEEE Trans. On Computers*, vol. C-22, no. 12, Dec. 1973.

[28] K. S. Fu, *Syntactic Methods in Pattern Recognition*. New York, NY: Academic Press, 1974.

[29] King-Sun Fu, *Syntactic Pattern Recognition Applications*. Berlin, NY: Springer-Verlag, 1977.

[30] F.T. Gamble, L.M. Frye, and D.R. Grieser, "Real-time Fingerprint Verification System," *Applied Optics*, vol. 31, no. 5, pp. 652 - 655, Feb. 1992.

[31] Rafael C. Gonzalez and Michael G. Thomason, "Syntactic Pattern Recognition, An Introduction," *IEEE PAMI*, vol. PAMI-3, no. 3, pp. 351 - 352, May 1981.

[32] Amara Graps, "An Introduction to Wavelets," *IEEE Computational Science and Engineering*, vol 2. no. 2, Summer 1995.

[33] A. Grasselli and Ed. S. Watanable, *Methodologies of Pattern Recognition*. New York, NY: Academic Press, 1968.

[34] Sir Edward Richard Henry, *Classification and Uses of Finger Prints*. London: Henry Majesty's Stationery Office (HMSO), 4th Issue, 1913.

[35] Sir Edward Richard Henry, *Classification and Uses of Finger Prints*. London: Henry Majesty's Stationery Office (HMSO), 7th Issue, 1934.

[36] Andrew K. Hrechak and James A. McHugh, "Automated Fingerprint Recognition using Structural Matching," *Pattern Recognition*, vol. 23, no. 8, pp. 893 - 904, 1990.

[37] Ching-Yu Huang, D. C. Hung and Jane H. Cheng, "The SPFL-Graph with Pattern Modeling of Fingerprints," in *Proc. Sixth Workshop on Digital Image Processing and Computer Graphics*, Oct. 1997.

[38] Ching-Yu Huang, D. C. Hung and Jane H. Cheng, "On The Automatic Preprocessing of Fingerprints," submitted to *1998 IEEE Southwest Symposium on Image Analysis and Interpretation*, Apr. 1998.

[39] D. C. Douglas Hung, "Enhancement and Feature Purification of Fingerprint Images," *Pattern Recognition*, vol. 26, no. 11, pp. 1660 - 1671, 1993.

[40] D. C. Hung and Ching-Yu Huang "On The Detection of The Center of A Convergence," in *Proc. Second Asian Conf. on Computer Vision*, Dec. 1995.

[41] D. C. Hung and Ching-Yu Huang, "A Model for Detecting Singular Points of a Fingerprint," in *Proc. 9th Florida Artificial Intelligence Research Symposium (FLAIRS'96)*, pp. 44 - 448, May 1996.

[42] D. C. Hung, Ching-Yu Huang and Jane H. Cheng, "A New Model for Representing and Retrieving Structural Patterns,", *Proc. The 5th International Conference on Intelligent Systems (IS'96)*, pp. 98 - 101, June 1996.

[43] D. C. Hung, Ching-Yu Huang and Jane H. Cheng, "Detecting Fingerprint Singular Points by A Hierarchical Model,", *Proc. 7th International Conference on Signal Processing Applications & Technology (ICSPAT'96)*, pp. 1153 - 1157, Oct. 1996.

[44] D. C. Hung, Ching-Yu Huang and Jane H. Cheng, "A Fuzzy Technique for Flow Oriented Image Direction Computing," in *Proc. Artificial Neural Networks in Engineering (ANNIE'96)*, pp. 519 - 524, Nov. 1996.

[45] D.K. Isenor and S.G. Zaky, "Fingerprint Identification using Graph Matching," *Pattern Recognition*, vol. 19, no. 2, pp. 113 - 122, 1986.

[46] Anil K. Jain, Nalini K. Ratha and Sridhar Lakshmanan, "Object Detection Using Gabor Filters," *Pattern Recognition*, vol. 30, no. 2, pp. 295 - 309, 1997.

[47] Ben-Kwei Jang and Roland T. Chin, "Analysis of Thinning Algorithms Using Mathematical Morphology," *IEEE PAMI*, vol. 12, no. 6, pp. 541 - 551, June 1990.

[48] Ben K. Jang and Roland T. Chin, "One pass Parallel Thinning: Analysis, Properties, and Quantitative Evaluation," *IEEE PAMI*, vol. 14, no. 11, pp. 1129 - 1140, Nov. 1992.

[49] Kalle Karu and Anil K. Jain, "Fingerprint Classification," *Pattern Recognition*, vol. 29, no. 3, pp. 389 - 404, Mar. 1996.

[50] Michael Kass and Andrew Witkin, "Analyzing Oriented Patterns," *Comput. Vision, Graphics, Image Processing: Image Understanding (CVGIP)*, 37, pp. 362 - 385, 1987.

[51] Masahiro Kawagoe and Akio Tojo, "Fingerprint Pattern Classification," *Pattern Recognition*, vol. 17, no. 3, pp. 295 - 304, 1984.

[52] Misao Kawashima and Kazho KIJI, "Personal Identification by Fingerprint or Palm-print," *Information Processing*, vol. 25, bo. 6, pp. 599-605, 1984.

[53] Jack Koplowitz and Stephen Plante, "Corner Detection for Chain Coded Curves," *Pattern Recognition*, vol. 28, no. 6, pp. 843 - 852, 1995.

[54] Hon Keung Kwan, "A Fuzzy Neural Network and its Application to Pattern Recognition," *IEEE Trans. Fuzzy Systems*, vol. 2, no. 3, pp. 185 - 193, Aug. 1994,

[55] Louisa Lam, Seong-Whan Lee and Ching Y. Suen, "Thinning Methodologies - A Comprehensive Survey," *IEEE PAMI*, vol. 14, no. 9, pp. 869 - 885, Sept. 1992.

[56] Edward T. Lee, "Fuzzy Tree Automata and Syntactic Pattern Recognition," *IEEE PAMI*, vol. PAMI-4, no. 4, pp. 445 - 449, July 1982.

[57] Henry C. Lee and R.E. Caenssien, "Advances in Fingerprint Technology," New York, NY: Elsevier, 1991.

[58] Seigo Lgaki, Shin Eguchi, Fumio Yamagishi, Hiroyuki Lkeda, and Takefumi Inagaki, "Real-time Fingerprint Sensor Using a Hologram," *Applied Optics, vol. 31, no. 11, pp. 1794 - 1802, Apr. 1992.*

[59] C. H. Lin, J. H. Liu, J. W. Osterberg and J. D. Nicol, "Fingerprint Comparison I: Similarity of Fingerprints," *J. Forensic Sci*, vol. 27, no. 2, pp. 290 - 304, Apr. 1982.

[60] C. H. Lin, J. H. Liu, J. W. Osterberg and J. D. Nicol, "Fingerprint Comparison II: On the Development of a Single Fingerprint Filing and Searching System," *J. Forensic Sci*, vol. 27, no. 2, pp. 305 - 317, Apr. 1982.

[61] Wei-Chung Lin and Richard C. Dubes, "A Review of Ridge Counting in Dermatoglyphics," *Pattern Recognition*, vol. 16, no. 1, pp. 1 - 8, 1983.

[62] Dario Maio, Davide Maltoni and Stefano Rizzi, "An efficient approach to on-line Fingerprint Verification," *VIII Int'l Symp. on Artificial Intelligence*, Mexico, Oct. 1995.

[63] Dario Maio and Davide Maltoni, "A Structural Approach to Fingerprint Classification," in *Proc. 13th ICPR*, 1996.

[64] Dario Maio and Davide Maltoni, "Direct Gray-Scale Minutiae Detection In Fingerprints," *IEEE PAMI*, Jan. 1997.

[65] James A. McHugh, *Algorithmic Graph Theory*. Englewood Cliffs, NJ: Prentice Hall, 1990.

[66] B.M. Mehtre, N. N. Murthy and S. Kapoor, "Segmentation of Fingerprint Images using the Directional Image," *Pattern Recognition*, vol.20, no. 4, pp. 429 - 435, 1987.

[67] B. M. Mehtre, "Segmentation of Fingerprint Images - A Composite Method," *Pattern Recognition*, vol. 22, no. 4, pp. 381 - 385, 1989.

[68] B. M. Mehtre, "Fingerprint Image Analysis for Automatic Identification," *Machine Vision and Application*, no. 6, pp. 124 - 139, 1993.

[69] B. Moayer and K. S. Fu, "A Syntactic Approach to Fingerprint Pattern Recognition" *Pattern Recognition*, vol. 7, pp. 1 - 23, 1975.

[70] B. Moayer and K. S. Fu, "An Application of Stochastic Languages to Fingerprint Pattern Recognition," *Pattern Recognition*, vol. 8, pp. 173 - 179, 1976.

[71] Bijan Moayer and King-Sun Fu, "A Tree System Approach for Fingerprint Pattern Recognition," *IEEE PAMI*, vol. 8, no. 3, pp 376 - 387, May 1986.

[72] Wayne Niblack, Phillip B. Gibbons and David Capson, "Generating Connected Skeletons for Exact and Approximate Reconstruction," *IEEE Pattern Recognition Conference*, pp. 826 - 828, 1992.

[73] Lawrence O'Gorman and Jeffrey V. Nickerson, "An Approach to Fingerprint Filter Design," *Pattern Recognition*, vol. 22, no. 1, pp. 29 - 38, 1989.

[74] Carol M. Orange and Erans C.A. Groen, "Model Based Corner Detection," in *Proc. IEEE Pattern Recognition Conf.*, pp. 690 - 691, 1993.

[75] Nikhil R. Pal and James C. Bezdek, "Measuring Fuzzy Uncertainty,", *IEEE Trans. on Fuzzy Systems*, vol. 2, no. 2, pp. 107 - 118, May 1994,

[76] F. Pernus, S. Kovacic and L. Gyergyek, "Minutiae based Fingerprint Recognition," in *Proc. 5th int. Conf. Pattern Recognition*, pp. 1380-1382, 1980.

[77] Xiao Qinghan, Dong Xiaoxue and Li Zhaoyu, "A recognition method for Fingerprint," *ACTA Automatica Sinica*, vol. 10, no. 1, pp. 69 - 73, 1984.

[78] Xiao Qinghan and Bian Zhaoqi, "An approach to fingerprint identification by using the attributes of feature lines of fingerprint," in *Proc. IEEE Conf. on Pattern Recognition*, pp. 663 - 665, 1986.

[79] C. V. Kameswara Rao, B. Prasad and K. R. Sharma, "An Automatic Fingerprint Classification System," in *Proc. 2nd Int. Conf. On Pattern Recognition*, pp. 180 - 184, 1974.

[80] C. V. Kameswara Rao, K. Balck, "Finding the Core Point in a Fingerprint," *IEEE trans. Comput.*, vol. C-27, pp. 77 - 81, Jan. 1978.

[81] C. V. Kameswara Rao, "On Fingerprint Pattern Recognition," *Pattern Recognition*, vol. 10, pp. 15 - 18, 1978.

[82] Kameswara Rao and Kenneth Balck, "Type Classification of Fingerprints: A Syntactic Approach," *IEEE PAMI*, vol. PAMI-2, no. 3, pp. 223 - 231, May 1980.

[83] Nailini K. Ratha, Shaoyun Chen and Anil K. Jain, "Adaptive Flow Orientation-Based Feature Extraction in Fingerprint Images," *Pattern Recognition*, vol. 28, no. 11, pp. 1657 - 1672, Nov. 1995.

[84] Paul L. Rosin, Alan C. F. Colchester and David J. Hawkes, "Early Image Representation using Regions Defined by Maximum Gradient Paths Between Singular Points," *Pattern Recognition*, vol. 25, no. 7, pp. 695 - 711, 1992.

[85] Peter T. Sander and Steven W. Zucker, "Singularities of Principal Direction Fields from 3-D Images," *IEEE PAMI*, vol. 14, no. 3, pp. 309 - 317, Mar. 1992.

[86] B. G. Sherlock and D. M. Monro, "A Model for Interpreting Fingerprint Topology," *Pattern Recognition*, vol. 26, no. 7, pp. 1047 - 1055, 1993.

[87] Alex Sherstinsky and Rosalind W. Picard, "Restoration and Enhancement of Fingerprint Images Using M-Lattice - A Novel Non-Linear Dynamical System," in *Proc. IEEE Conf. on Pattern Recognition*, pp. 195 - 200, 1994.

[88] Frank Y. Shih and Wai-Tak Wong, "Fully Parallel Thinning with Tolerance to Boundary Noise," *Pattern Recognition*, vol. 27, no. 12, pp. 1677 - 1695, 1994.

[89] Chiao-Fe Shu and Ramesh C. Jain, "Direct Estimation and Error Analysis for Oriented Patterns," *Computer Vision Graphics and Image Processing*, vol. 58, no. 3, pp. 383 - 398, Nov. 1993.

[90] Chiao-Fe Shu and Ramesh C. Jain, "Vector Field Analysis for Oriented Patterns," *IEEE PAMI*, vol. 16, no. 9, pp. 946 - 950, Sept. 1994.

[91] Dave Sims, "Decriminalizing The Fingerprint," *IEEE Computer Graphics and Applications*, pp. 15 - 16, July 1994.

[92] M. K. Sparrow and P. J. Sparrow, "A Topological Approach to the Matching of Single Fingerprints: Development of Algorithms for use on Rolled Impressions," INational Bureau of standards Special Publication 500 - 124, U.S. Goverment Printing Office, Washington, D.C., 1985.

[93] M. K. Sparrow and P. J. Sparrow, "A Topological Approach to the Matching of Single Fingerprints: Development of Algorithms for use on Latent Impressions," National Bureau of standards Special Publication 500 - 126, U.S. Goverment Printing Office, Washington, D.C., 1985.

[94] V. S. Srinivasan and N. N. Murthy, "Detection of Singular Points in Fingerprint Images," *Pattern Recognition*, vol. 25, no. 2, pp. 139 - 153, 1992.

[95] D. A. Stoney and J. I. Thornton, "A Critical Analysis of Quantitative Fingerprint Individuality Models," *J. Forensic Sci*, 31, pp. 1187 - 1216, 1986.

[96] Thomas A. Sudkamp, *Languages and Machines*. Reading, MA: Addison Wesley, 1988.

[97] S. Tabbone and D, Ziou, "Efficient Edge Detection Using Two Scales," in *Proc. IEEE Pattern Recognition Conf.*, pp. 789 - 790, 1993.

[98] Hai Tai and Zhaoqi Bian, "An Orientation Normalized Vector Quantizer for Flow-like Image Coding," in *Proc. IEEE Pattern Recognition Conf.*, pp. 465 - 470, 1993.

[99] Masahiro Takeda, Saatoshi Uchida, Kenichi Hiramatsu, and Tokumi Mastunami, "Finger Image Identification Method for Personal Verification," in *Proc. IEEE Pattern recognition Conf.*, pp. 761 - 766, 1990.

[100] C.L. Tan and S. K. K. Loh, "Efficient Edge Detection Using Hierarchical Structures," *Pattern Recognition*, vol. 26, no. 1, pp. 127 - 135, 1993.

[101] M.R. Verma, A.K. Majumdar and B. Chatterjee, "Edge Detection in Fingerprints," *Pattern Recognition*, vol. 20, no. 5, pp. 513 - 523, 1987.

[102] David Vernon, "Automatic Detection of Secondary Creases in Fingerprints," *Optical Engineering*, vol. 32, no. 10, pp. 2616 - 2623, Oct. 1993.

[103] Pedro R. Vizcaya and Lester A. Gerhardt, "A Nonlinear Orientation Model for Global Description of Fingerprints," *Pattern Recognition*, vol. 29, no. 7, pp. 1221 - 1231, 1996.

[104] C. I. Watson, G. T. Candela and P. J. Grother, "Comparision of FFT Fingerprint Filtering Methods for Neural Network Classification," National Institute of Standards and Technology (NIST) Technical Report 5493, Image Recognition Group, Advanced Systems Division, NIST, US Dept. of Commerce, Aug. 1994.

[105] J. H. Wegstein, "Manual and automated fingerprint registration," Tech. Note 730, National Bureau of Standards, June 1972.

[106] J. J. Wegstein, "An Automated Fingerprint Identification System," National Bureau of Standards Special Publication 500 - 89, U.S. Goverment Printing Office, Washington, D.C., 1982.

[107] T. F. Wilson and P. L. Woodard, "Automated Fingerprint Identification Systems: Technology and Policy Issues," Bureau of Justice Statistics Report, U.S. Goverment Printing Office, Washington, D.C., 1987.

[108] C. L. Wilson, G. T. Candela and C. I. Watson, "Neural Network Fingerprint Classification," *Journal Artifical Neural Network*, No. 2, pp. 1 - 25, 1993.

[109] Qinghan Xiao and Hazem Raafat, "Fingerprint Image Postprocessing: A Combined Statistical and Structural Approach," *Pattern Recognition*, vol. 24, no. 10, pp. 985 - 992, 1991.

[110] Steven W. Zucker, "Early Orientation Selection: Tangent Fields and the Dimensionality of Their Support," *Computer Vision Graphics and Image Processing (CVGIP)*, vol. 32, pp. 74 - 103, 1985.